Supporting Information for

Bio-Inspired Bimetallic Models for Electrochemical CO_2 Reduction

Weifang Feng,[a] Ying Xiong,[a] Ping Zhang,[a] Minghong Li,[a] Yaping Zhang,[a] Fei Li[*b] and Lin Chen*[*a]*

[a] State Key Laboratory of Environment-Friendly Energy Material, School of Materials and Chemistry, Southwest University of Science and Technology, Mianyang 621010, P. R. China

[b] State Key Laboratory of Fine Chemicals, Dalian University of Technology, Dalian 116024, P. R. China

Corresponding Authors

Email*: chenlin101101@aliyun.com

Email*: lifei@dlut.edu.cn

Contents

1. Figure Contents

2. Table Contents

3. Scheme Contents

4. Materials and Instruments

All manipulations for preparation and handling of organometallic complexes were carried out under Ar. All the solvents were used as received. Other commercially available chemicals such as $Re(CO)_5Cl$, $Pd(PPh_3)_4$, 6-bromo-2,2'-bipyridine, sulfurous dichloride, 1,4,7,10,13-pentaoxa-16-azacyclooctadecane, sodium hydroxide, toluene, potassium carbonate, anhydrous methanol and were purchased from local suppliers and used as received. Water was deionized with the Millipore Milli-Q UF Plus system. Glass carbon disc (3 mm), Ag^+/Ag electrode and platinum wire were purchased from CHI for electrochemical studies.

NMR Spectra were collected with a varian INOVA 600 NMR spectrometer. Mass spectra were recorded with HP 1100 HPL/ESI-DAD-MS and Waters/Micromass LC/Q-TOF-MS instruments. Elemental analyses were performed with a Thermoquest-Flash EA 1112 elemental analyzer.

5. Crystallographic Structure Determinations

The single-crystal X-ray diffraction data were collected with an Bruker Smart Apex II CCD diffractometer with agraphite-monochromated Mo-K radiation (= 0.071073 Å) at 296 K using the θ-2 scan mode. Data processing was accomplished with the SAINT processing program. Intensity data were corrected for absorption by the SADABS program. All structures were solved by direct methods and refined on F^2 against full-matrix least-squares methods by using the SHELXTL 97 program package. All non-hydrogen atoms were refined anisotropically. Hydrogen atoms were located by geometrical calculation. Crystallographic data and selected bond lengths and angles for **1** are given in Table S1-S3. **CCDC-2289719** contain the supplementary crystallographic data for this paper. These data can be obtained free of charge from The Cambridge Crystallographic Data Centre via *www.ccdc.cam.ac.uk/data_request/cif*.

6. Electrochemistry Study Details

Cyclic voltammetry (CV): Cyclic voltammetry experiments were carried out in a three-electrode cell under high-purity Ar (99.999%) or CO_2 (99.99%) using CHI 760E potentiostat. The working electrode was a glassy carbon disc (diameter 3 mm) polished with 0.5-mm diamond pastes, then sonicated in ion-free water for 15 min and washed with MeCN prior to use. The reference electrode was a Ag^+/Ag (0.01 M $AgNO_3$) electrode and the counter electrode was platinum wire. Rhenium complex concentrations were generally at 0.5 mM. A solution of 0.1 M $^nBu_4NPF_6$ (Fluka, electrochemical grade) in CH_3CN was used as supporting electrolyte, which was degassed by bubbling with dry Ar or CO_2 for 5 min before measurement. The catalytic experiments with CO_2 were performed in CO_2-saturated CH_3CN solution (about 0.28 M) with addition of a certain amount of KPF_6. The scan rate is 100 mV/s. Ferrocene (Fc) was added as an internal reference in the end of each measurement to convert the measured potentials and ***all potentials given in this work are referred to*** $Fc^{+/0}$.

7. Fourier-Transform Infrared Reflectance Spectroelectrochemistry (FTIR-SEC)

A homemade FTIR-SEC instrument was used for this study. The cell consists of a glass carbon working electrode (10 mm), a Pt counter (15 mm × 30 mm) electrode, and a $Ag/AgNO_3$ reference electrode and a CaF_2 plate as the optical window. The IR beam is directed to focus on the working electrode through the optical window, where it is reflected and ultimately directed to the Bruker Vertex 80 detector. The dry CH_3CN solution (0.1 M TBAP) prepared under an atmosphere of Ar is used as the electrolyte.

8. Experiment section

General procedure for the preparation of the target ligands involved in this article.

The procedure was slightly modified according to the literature (Shuanglin He et. al. *Angew. Chem. Int. Ed*. **2023**, e202216082). An oven-dried Schlenk flask equipped with a stir bar was evacuated, back-filled with Ar, and charged with 1 equiv bromo-precursors, 1.1 equiv corresponding phenylboric acid, 0.05 equiv $Pd(PPh_3)_4$, toluene (50 mL), ethanol (50 mL) and an aqueous 2 M solution of potassium carbonate (12 mL). The solution was stirred at room temperature for 15 min before heated to 92 °C for 42 h, the mixture was cooled to room temperature and 30% hydrogen peroxide (0.4 mL) was added. The mixture was stirred at room temperature for 30 min, the product was extracted using diethyl ether (2 × 100 mL), and the extract was washed with saturated sodium chloride solution (1 × 30 mL) and water (3 × 30 mL) to give a red organic layer. Following drying with magnesium sulfate, the volatiles were removed under reduced pressure to give an orange-brown residue. The residues of ligand were removed using a short silica gel column employing dichloromethane as eluting solvent. After the solvent was removed under reduced pressure, the product was obtained as a solid.

Synthesis of ligand L_1

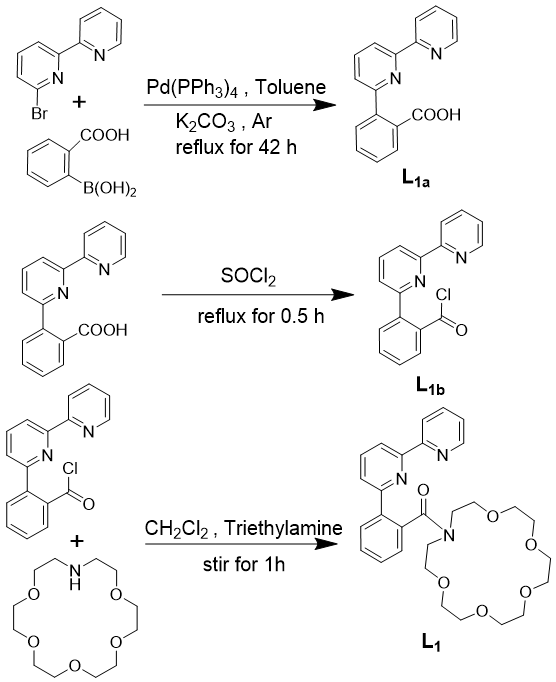

Scheme S 1 preparation of target ligand L_1.

The 2-([2,2'-bipyridin]-6-yl)benzoic acid (**L_{1a}**) was obtained according to literature procedures (Shuanglin He et. al. *Angew. Chem. Int. Ed*. **2023**, e202216082). The reaction is monitored by TLC (R*f* = 0.3, MeOH : DCM = 1 : 9).

2-([2,2'-bipyridin]-6-yl)benzoyl chloride (**L_{1b}**) was prepared by stirring a mixture of **L_{1a}** (1.90 g, 6.88 mmol) and thionyl chloride (10.00 mL) mixing for 0.5 h. After the reaction, the volatiles were removed under reduced pressure to give the **L_{1b}**. the dichloromethane solution of 1,4,7,10,13-pentaoxa-16-azacyclooctadecane (2.20 g, 8.32 mmol) was added to **L_{1b}**, and triethylamine (1.00 mL) was slowly added. The mixture was stirred at room temperature for 1 h. Quenched reaction with water and collected organic layer of the product. Finally, the product was purified by silica gel column chromatography (dichloromethane) to obtain the target ligand **L_1** (1.60 g, 3.07 mmol, 44.62% yield)and the reaction is monitored by TLC(Rf = 0.5, MeOH : DCM = 1 : 9).: ^{1}H NMR (600 MHz, DMSO) δ 8.70-8.65 (1H, d), 8.56 (1H, d), 8.41 (1H, d), 7.90-7.82 (2H, m), 7.77 (1H, d), 7.67 (1H, d), 7.50 (1H t), 7.46 (1H, t), 7.43 (1H, d), 7.33-7.29 (1H, t), 3.66 (2H, m), 3.60-3.29 (20H, m), 3.23 (2H, m). ESI-MS: Calcd for $[M + H^+]^+$: m/z 522.25; found: 522.22.

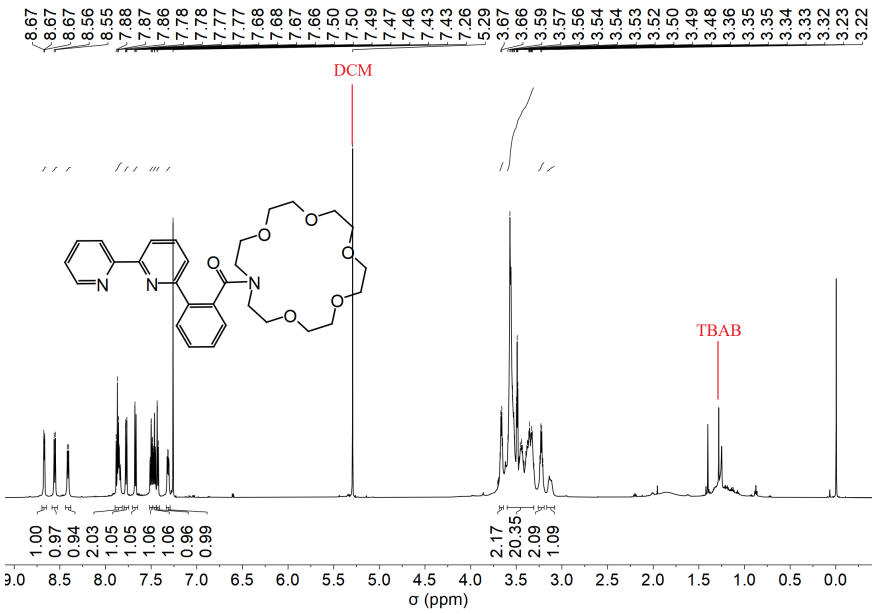

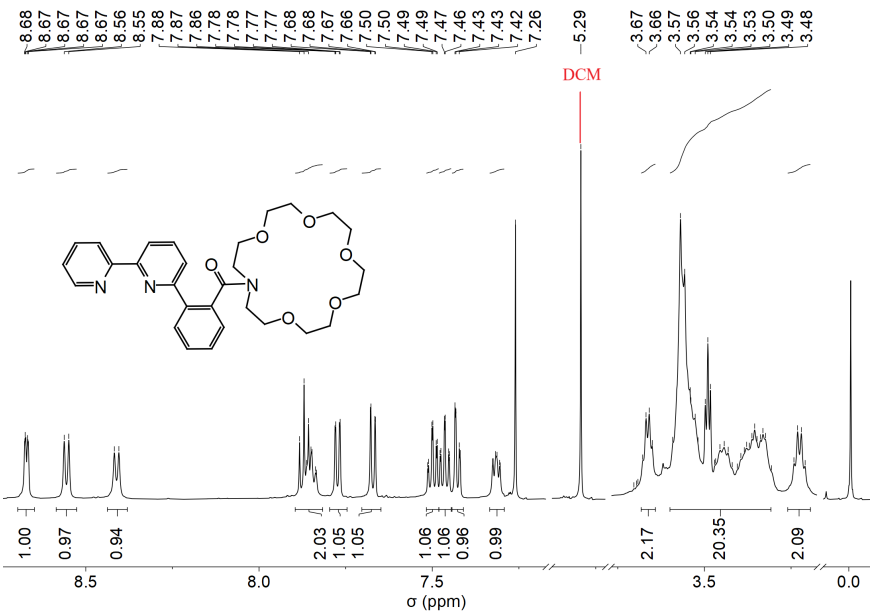

Figure S 1 ^{1}H NMR (Chloroform, 600 MHz) spectrum of $\mathbf{L_1}$.

Synthesis of ligand L_2

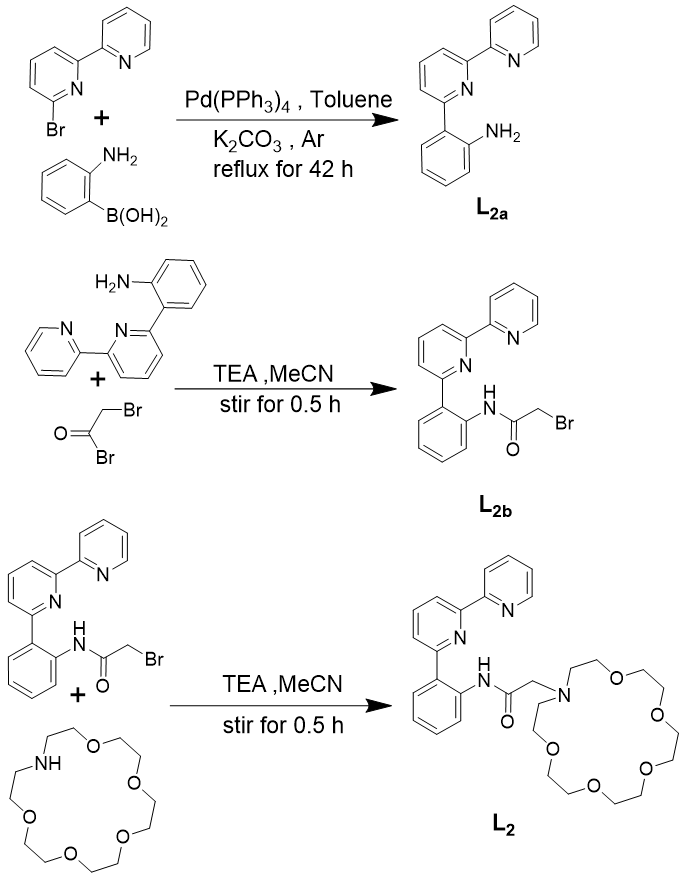

Scheme S 2 preparation of target ligand L_2.

2-([2,2'-bipyridin]-6-yl)aniline (L_{2a}) was obtained according to literature procedures (Shuanglin He et. al. *Angew. Chem. Int. Ed.* **2023**, e202216082).The reaction is Monitored by TLC (R*f* = 0.4, MeOH : DCM = 1 : 9).

N-(2-([2,2'-bipyridin]-6-yl)phenyl)-2-bromoacetamide (L_{2b}) was prepared by stirring an acetonitrile solution of a mixture of L_{2a} (1.00 g, 4.05 mmol) and 2-bromoacetyl bromide (4.05 mmol) for 0.5 h, and triethylamine (1.00 mL) was slowly added. After the reaction, 1,4,7,10,13-pentaoxa-16-azacyclooctadecane (1.30 g, 4.92 mmol) was added to L_{2b} and triethylamine (1.00 mL) was slowly added. The mixture was stirred at room temperature for 1 h. Quenched reaction with water and collected organic layer of the product. Finally, the product was purified by silica gel column chromatography (dichloromethane) to obtain the target ligand L_2 (0.90 g, 1.64 mmol, 40.49% yield) and the reaction is Monitored by TLC (R*f* = 0.4, MeOH : DCM = 1 : 9). **:** ^{1}H NMR (600 MHz, Chloroform) δ 11.01 (1H, s), 8.73 (1H, d), 8.50 (1H, d), 8.42 (2H,

d), 7.98 (1H, t), 7.85 (1H, t), 7.56 (2H, t), 7.46 (1H, t), 7.36 (1H, d), 7.24 (1H, t), 3.85-3.27 (20H, m), 3.20 (2H, d), 2.45 (4H, t) ESI-MS: Calcd for $[M + H^+]^+$: m/z 551.28; found: 551.22.

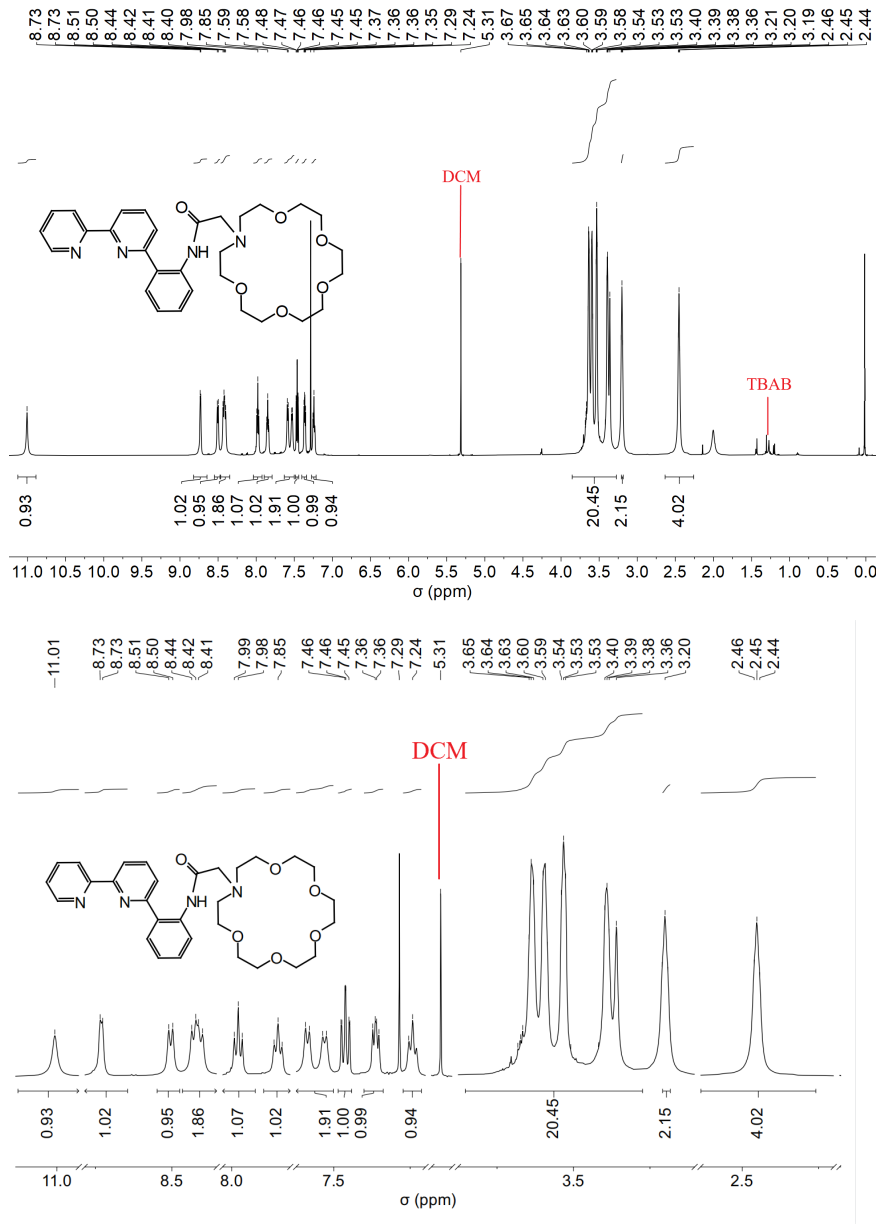

Figure S 2 ^{1}H NMR (Chloroform, 600 MHz) spectrum of $\mathbf{L_2}$.

Synthesis of ligand L_3

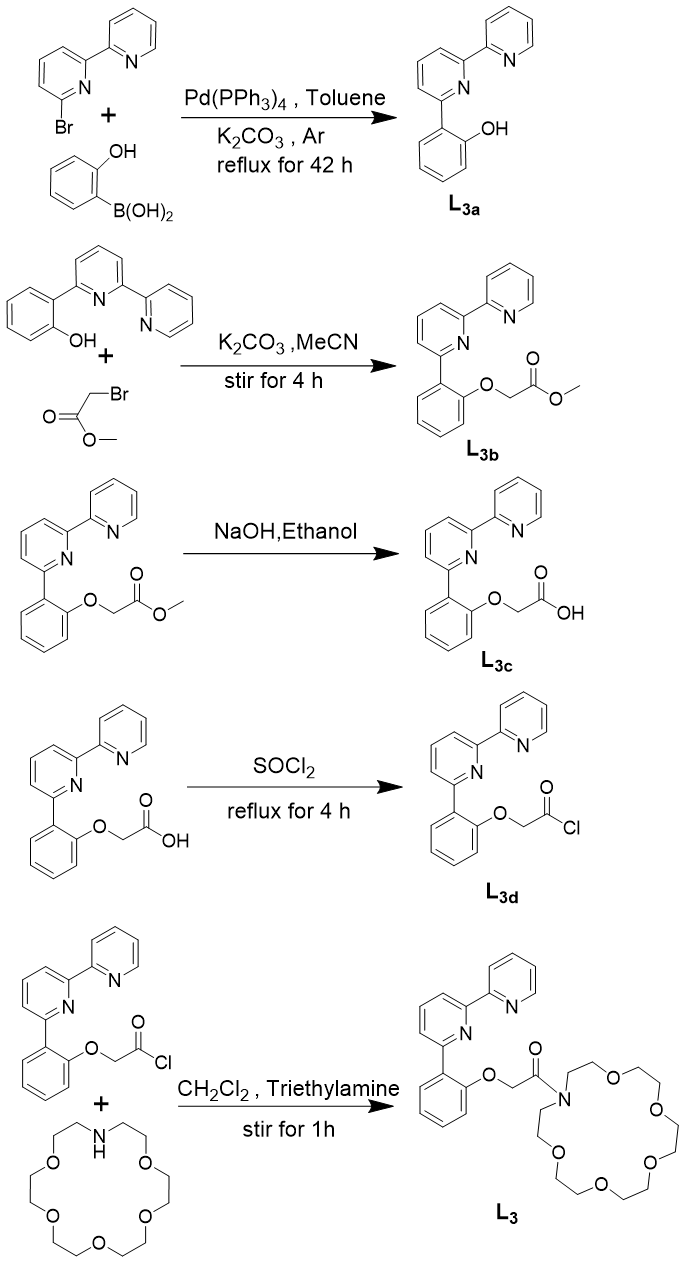

Scheme S 3 preparation of target ligand $\mathbf{L_3}$.

2-([2,2'-bipyridin]-6-yl)phenol ($\mathbf{L_{3a}}$) was obtained according to literature procedures (Shuanglin He et. al. *Angew. Chem. Int. Ed.* **2023**, e202216082). The reaction is monitored by TLC (R*f* = 0.4, MeOH : DCM = 1 : 4).

Methyl bromoacetate (4.43 mmol) and potassium carbonate (0.70 g, 5.06 mmol) were added to the acetonitrile (5.00 mL) solution of $\mathbf{L_{3a}}$ (1.10 g, 4.43 mmol), respectively, and stirred for 4h to obtain methyl 2-(2-([2,2'-bipyridin]-6-yl)phenoxy)acetate ($\mathbf{L_{3b}}$). Subsequently,

2-(2-([2,2'-bipyridin]-6-yl)phenoxy)acetic acid (**L_{3c},** 0.79 g, 2.58 mmol, 58.23% yield). was obtained by hydrolysis of **L_{3b}** and the reaction is monitored by TLC (R*f* = 0.6, MeOH : DCM = 1 : 9). 2-(2-([2,2'-bipyridin]-6-yl)phenoxy)acetyl chloride (**L_{3d}**) was prepared by stirring a mixture of **L_{3c}** and thionyl chloride (10.00 mL) mixing for 0.5 h. After the reaction, the volatiles were removed under reduced pressure to give the **L_{3d}** the dichloromethane solution of 1,4,7,10,13-pentaoxa-16-azacyclooctadecane (0.80 g, 3.03 mmol) was added to **L_{3d}**, and triethylamine (1.00 mL) was slowly added. The mixture was stirred at room temperature for 1 h. Quenched reaction with water and collected organic layer of the product. Finally, the product was purified by silica gel column chromatography (dichloromethane) to obtain the target ligand **L_3** (0.60 g, 1.09 mmol, 42.25% yield) and the reaction is Monitored by TLC (R*f* = 0.5, MeOH : DCM = 1 : 9)**:** ^{1}H NMR (600 MHz, Chloroform) δ 8.69 (1H, d), 8.58 (1H, d), 8.35 (1H, d), 8.15 (1H, d), 8.02 (1H, d), 7.88-7.81 (2H, m), 7.38-7.34 (1H, m), 7.33-7.30 (1H, m), 7.14 (1H, t), 7.04 (1H, d), 4.90 (2H, s), 3.68-3.65 (4H, m), 3.64-3.59 (16H, m), 3.57-3.54 (4H, m). ESI-MS: Calcd for [M + H$^+$]$^+$: m/z 552.26; found: 552.24.

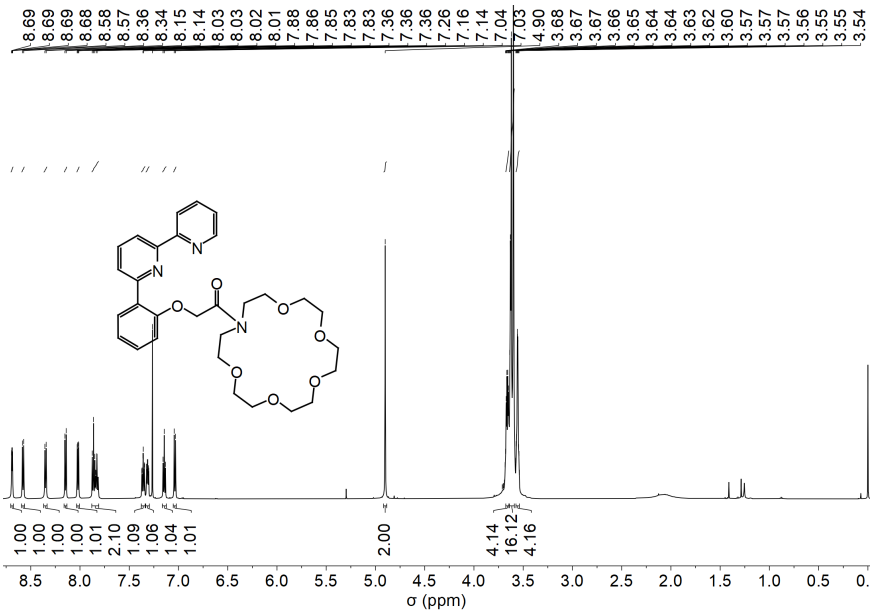

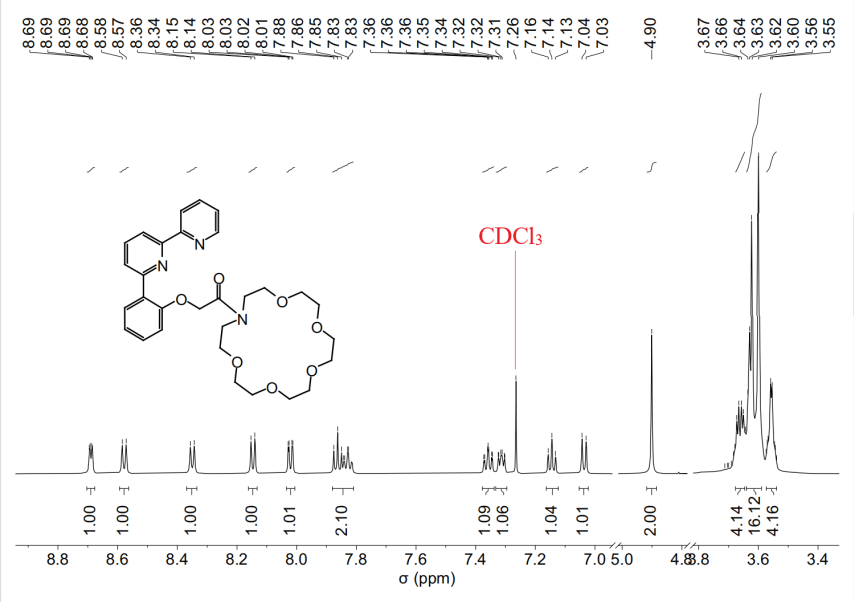

Figure S 3 ^{1}H NMR (Chloroform, 600 MHz) spectrum of **L_3**.

Synthesis of ligand L_4

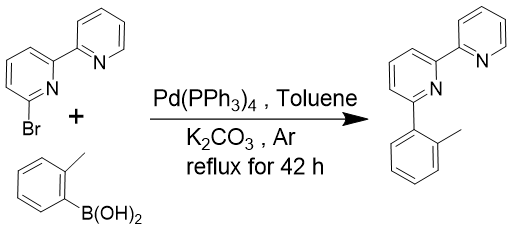

Scheme S 4 preparation of target ligand L_4.

6-(o-tolyl)-2,2'-bipyridine was obtained according to literature procedures (Shuanglin He et. al. *Angew. Chem. Int. Ed*. **2023**, e202216082). The reaction is Monitored by TLC (R*f* = 0.5, MeOH : DCM = 1 : 9): ^{1}H NMR (600 MHz, Chloroform) δ 8.70 (1H, d), 8.51 (1H, d), 8.40 (1H, d), 7.89 (1H, s), 7.81 (1H, s), 7.47 (2H, d), 7.36-7.18 (4H, m), 2.48 (3H, s). ESI-MS: Calcd for $[M + H^+]^+$: m/z 247.12; found: 247.14.

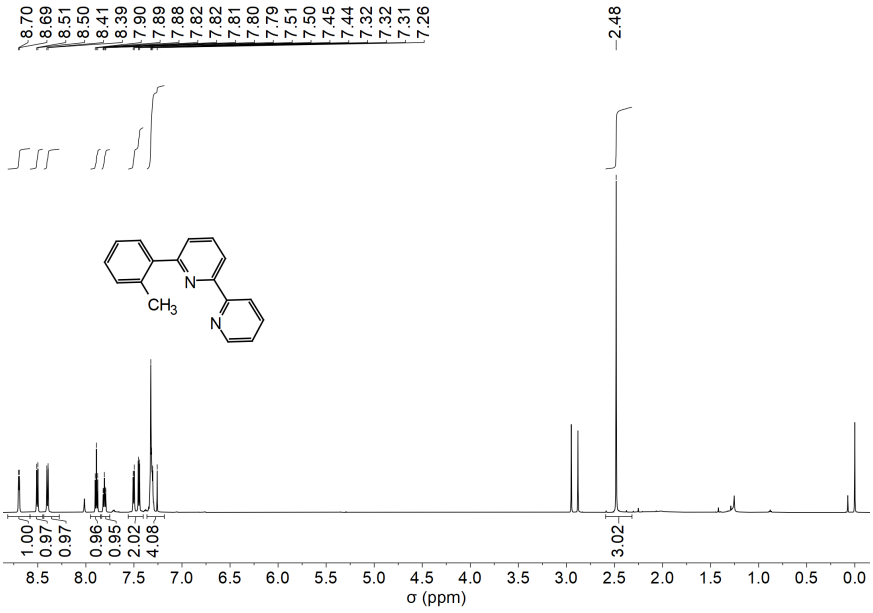

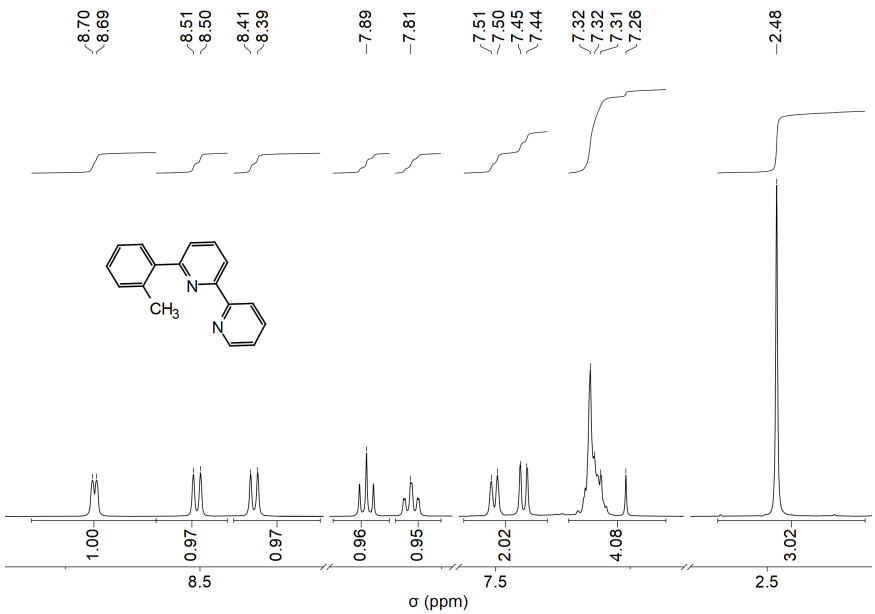

Figure S 4 ^{1}H NMR (DMSO, 600 MHz) spectrum of **L$_4$**.

Synthesis of complexes 1

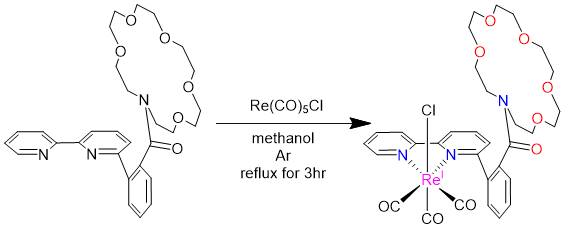

Scheme S 5 preparation of target complex **1.**

Preparation of complexes 1. Compound $Re(CO)_5Cl$ (0.13 g, 0.36 mmol) was added to a degassed methanol solution (2.00 mL) of 1 equiv $\mathbf{L_1}$. The resulting colorless solution was heated to reflux for 3 h under argon, then allowed to cool to room temperature before filtration. The filtrate was collected and concentrated, then washed with Et_2O and dried in vacuo to afford yellow product (0.25 g, 0.30 mmol, 83.33% yield). The following were observed for the mixture of atropisomers: ^{1}H NMR (600 MHz, Chloroform) δ 9.10 (1H, d), 8.28-7.83 (6H, m), 7.72-7.50 (4H, m), 4.03-3.29 (24H, m); IR (KBr, Figure S 13) ν_{CO}: 2021 (s), 1917 (s), 1892 (s) cm^{-1}; Anal. Calcd for **1**, C32H35ClN3O9Re: C, 46.46; H, 4.26; N, 5.08; found: C, 46.44; H, 4.22; N, 5.04; MS (TOF-ES): m/z = 792.1920 $[M - Cl^-]^+$, m/z = 850.1500 $[M+Na^+]^+$.

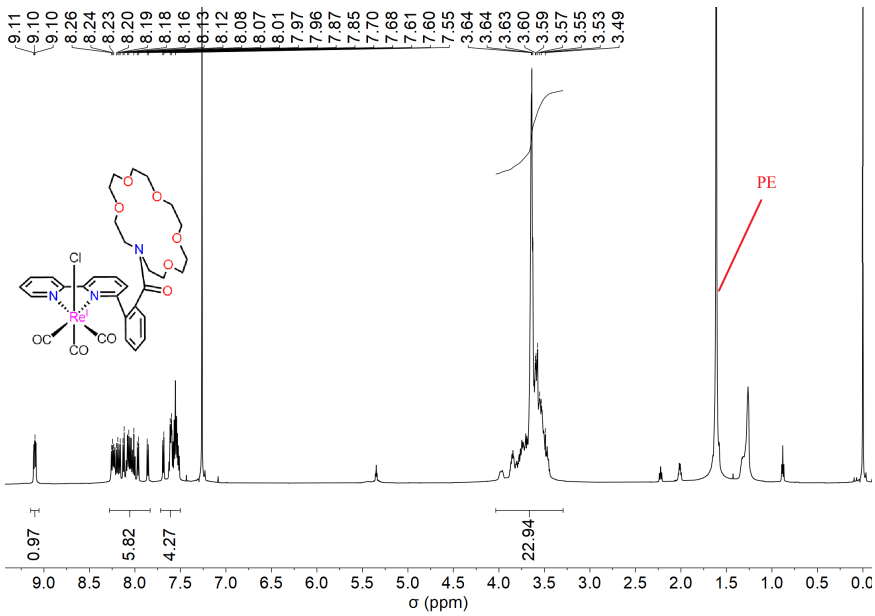

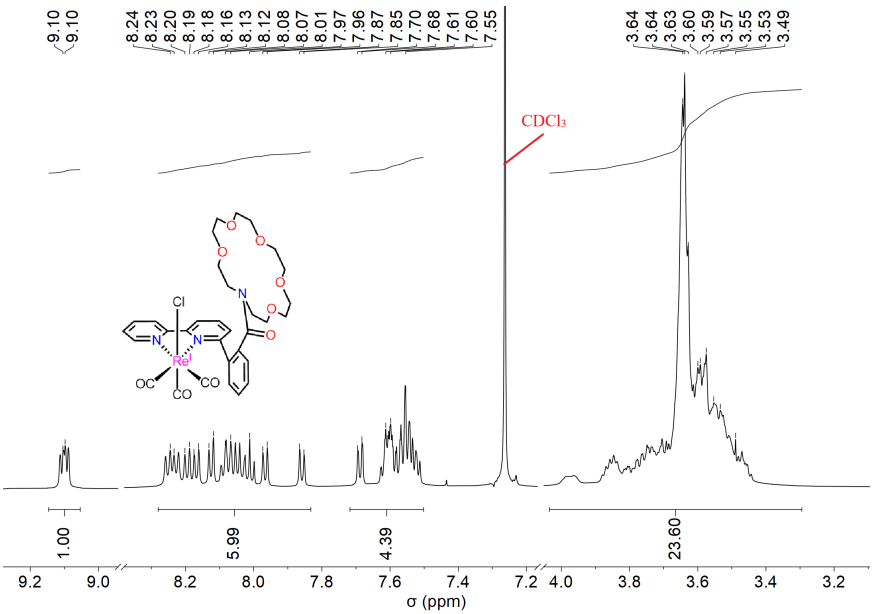

Figure S 5 ^{1}H NMR (Chloroform, 600 MHz) spectrum of **1**.

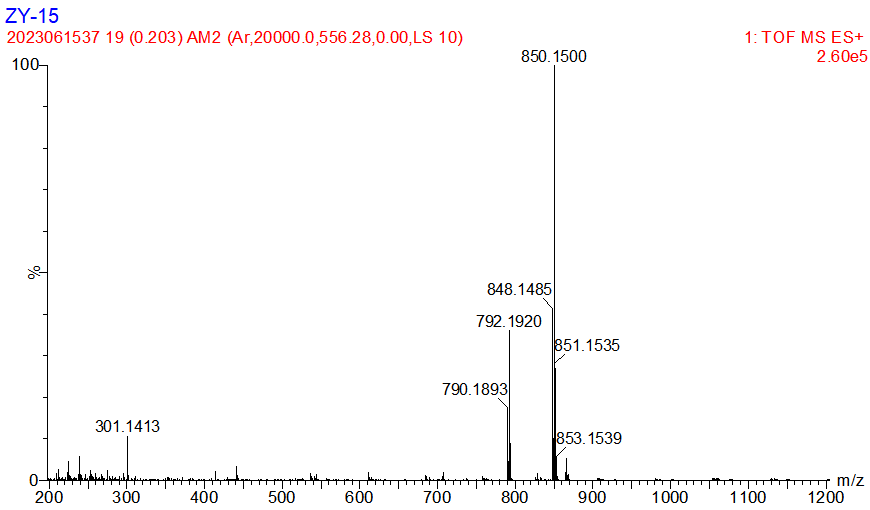

Figure S 6 high resolution mass spectrum of **1**.

Synthesis of complexes 2

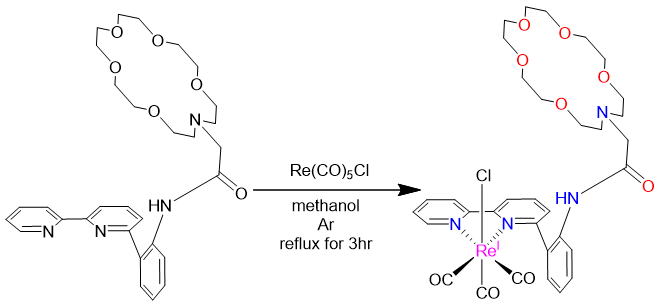

Scheme S 6 preparation of target complex **2**.

Preparation of complexes 2. Compound $Re(CO)_5Cl$ (0.10 g, 0.29 mmol) was added to a degassed methanol solution (2.00 mL) of 1 equiv $\mathbf{L_2}$. The resulting colorless solution was heated to reflux for 3 h under argon, then allowed to cool to room temperature before filtration. The filtrate was collected and concentrated, then washed with Et_2O and dried in vacuo to afford yellow product (0.20 g, 0.23 mmol, 79.31% yield). The following were observed for the mixture of atropisomers: ^{1}H NMR (600 MHz, Chloroform) δ 9.99 (1H, s), 9.31-8.98 (2H, m), 8.44-8.06 (4H, m), 7.68-7.28 (5H, m), 4.44-2.98 (24H, m), 2.64 (2H, d); IR (KBr, Figure S 13) ν_{CO}: 2025 (s), 1920 (s), 1904 (s) cm^{-1}; Anal. Calcd for **2**, $C_{33}H_{38}ClN_4O_9Re$: C, 46.29; H, 4.47; N, 6.54; found: C, 46.28; H, 4.46; N, 6.53; MS (TOF-ES): m/z = 821.2189 $[M - Cl^-]^+$, m/z = 857.1956 $[M+H^+]^+$, m/z = 879.1772 $[M+Na^+]^+$.

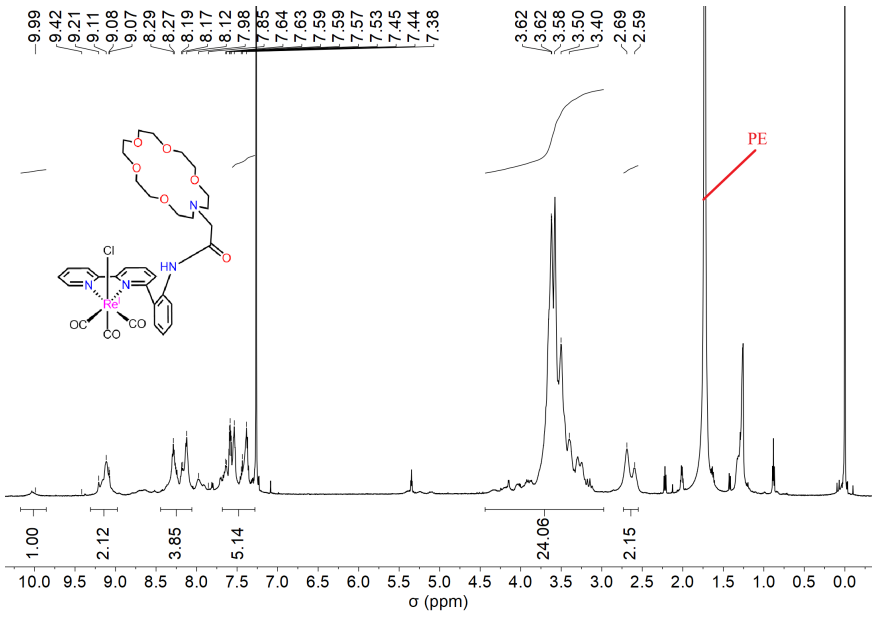

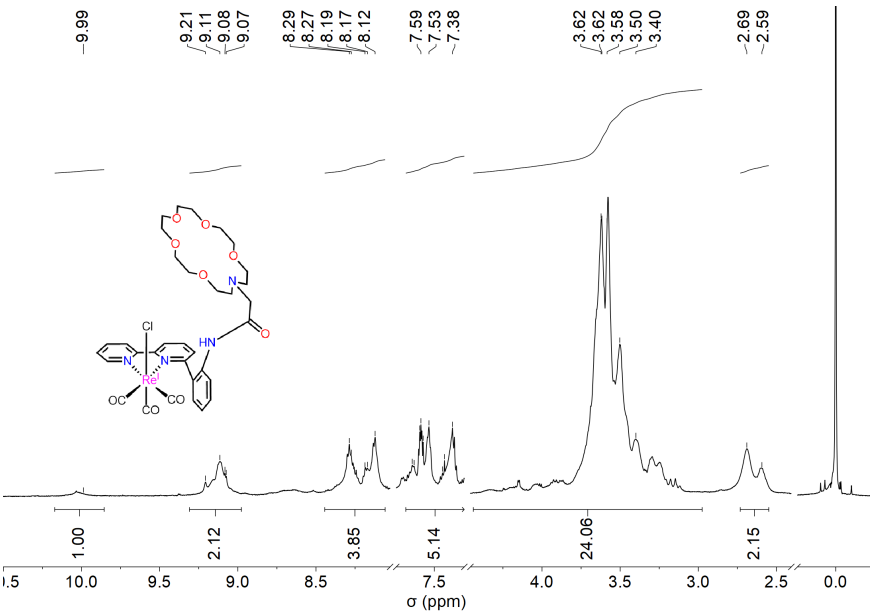

Figure S 7 ^{1}H NMR (Chloroform, 600 MHz) spectrum of **2**.

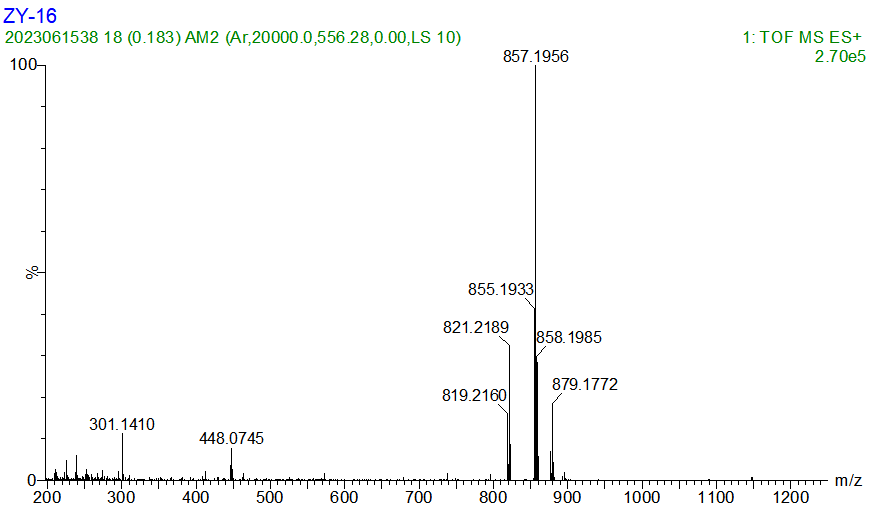

Figure S 8 high resolution mass spectrum of **2**.

Synthesis of complexes 3

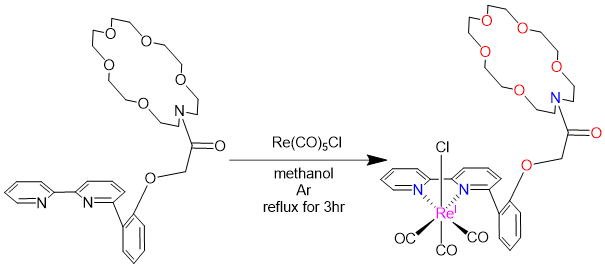

Scheme S 7 preparation of target complex **3**.

Preparation of complexes 3. Compound $Re(CO)_5Cl$ (0.11 g, 0.30 mmol) was added to a degassed methanol solution (2.00 mL) of 1 equiv $\mathbf{L_3}$. The resulting colorless solution was heated to reflux for 3 h under argon, then allowed to cool to room temperature before filtration. The filtrate was collected and concentrated, then washed with Et_2O and dried in vacuo to afford yellow product (0.20 g, 0.23 mmol, 76.66% yield). The following were observed for the mixture of atropisomers: ^{1}H NMR (600 MHz, Chloroform) δ 9.09 (1H, d), 8.26-8.14 (2H, m), 8.06-7.98 (4H, m), 7.53-7.37 (3H, m), 7.15 (1H, d), 5.06 (1H, d), 4.83 (1H, d), 3.89-3.40 (24H, m): IR (KBr, Figure S 13) ν_{CO}: 2021 (s), 1917 (s), 1892 (s) cm^{-1}; Anal. Calcd for **3**, C33H37ClN3O10Re: C, 46.23; H, 4.35; N, 4.90; found: C, 46.22; H, 4.33; N, 4.91; MS (TOF-ES): m/z = 822.2031 [M – Cl$^-$]$^+$, m/z = 880.1610 [M+Na$^+$]$^+$.

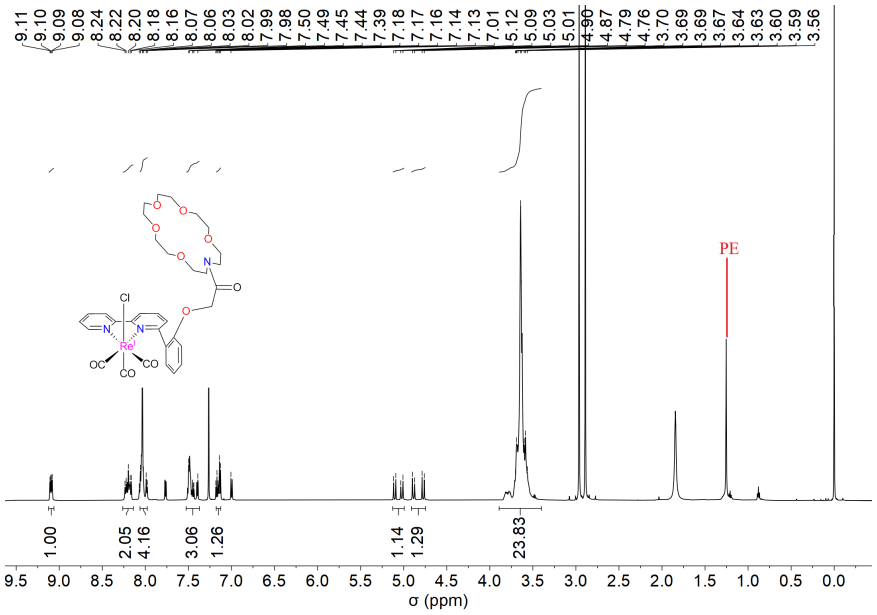

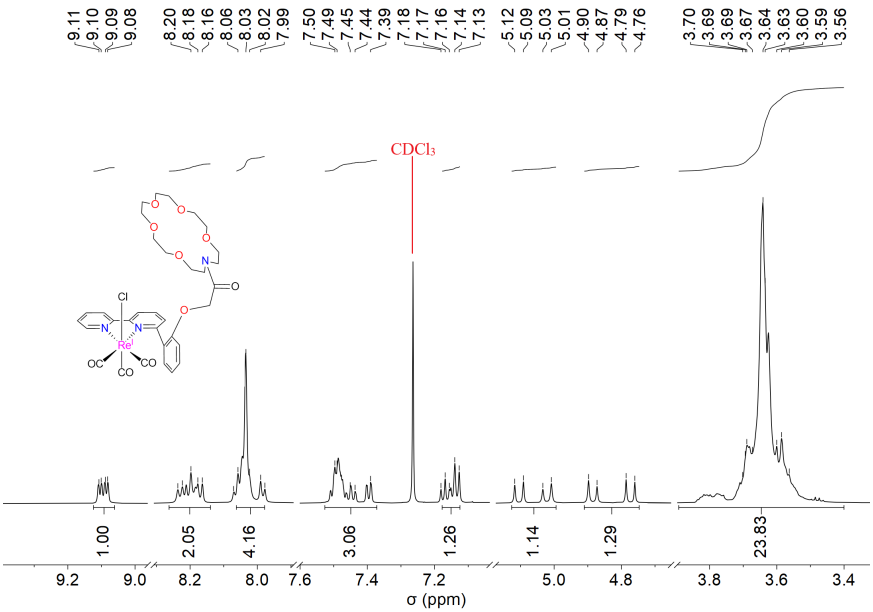

Figure S 9 ^{1}H NMR (Chloroform, 600 MHz) spectrum of **3**.

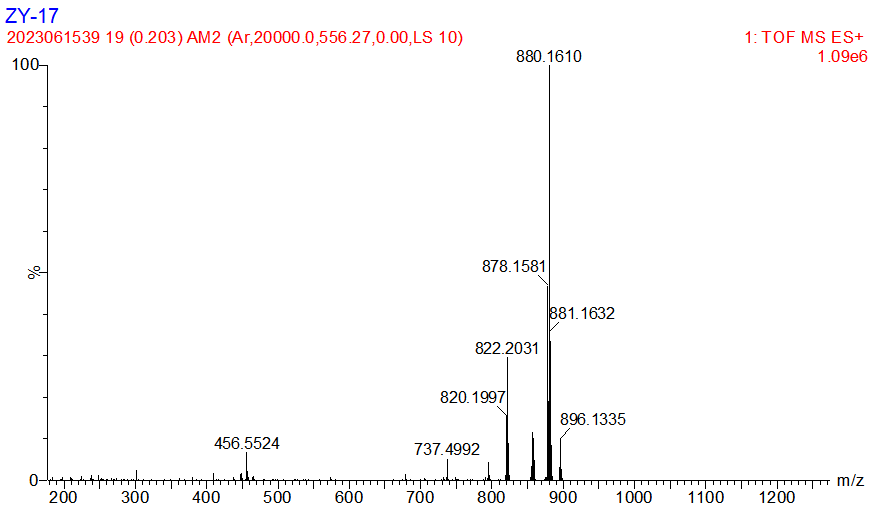

Figure S 10 high resolution mass spectrum of **3**.

Synthesis of complexes 4

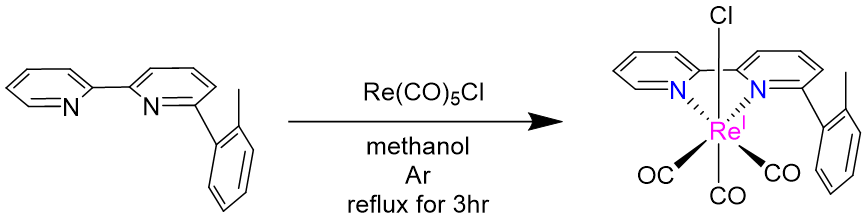

Scheme S 8 preparation of target complex **4**.

Preparation of complexes 4. Compound $Re(CO)_5Cl$ (0.10 g, 0.28 mmol) was added to a degassed methanol solution (2.00 mL) of 1 equiv $\mathbf{L_4}$. The resulting colorless solution was heated to reflux for 3 h under argon, then allowed to cool to room temperature before filtration. The filtrate was collected and concentrated, then washed with Et_2O and dried in vacuo to afford yellow product (0.12 g, 0.22 mmol, 78.57% yield). The following were observed for the mixture of atropisomers: ^{1}H NMR (600 MHz, Chloroform) δ 9.11 (1H, t), 8.29-8.19 (2H, m), 8.07 (2H, d), 7.56-7.44 (3H, m), 7.37 (2H, t), 7.27 (1H, d), 2.32 (2H, s), 2.22 (1H, s); IR (KBr, Figure S 13) ν_{CO}: 2023 (s), 1917 (s), 1895 (s) cm^{-1}; Anal. Calcd for **4**, C20H14ClN2O3Re: C, 43.52; H, 2.56; N, 5.07; found: C, 43.55; H, 2.51; N, 5.05; MS (TOF-ES): m/z = 517.0560 $[M - Cl^-]^+$, m/z = 575.0141 $[M+Na^+]^+$, m/z = 590.9879 $[M+K^+]^+$.

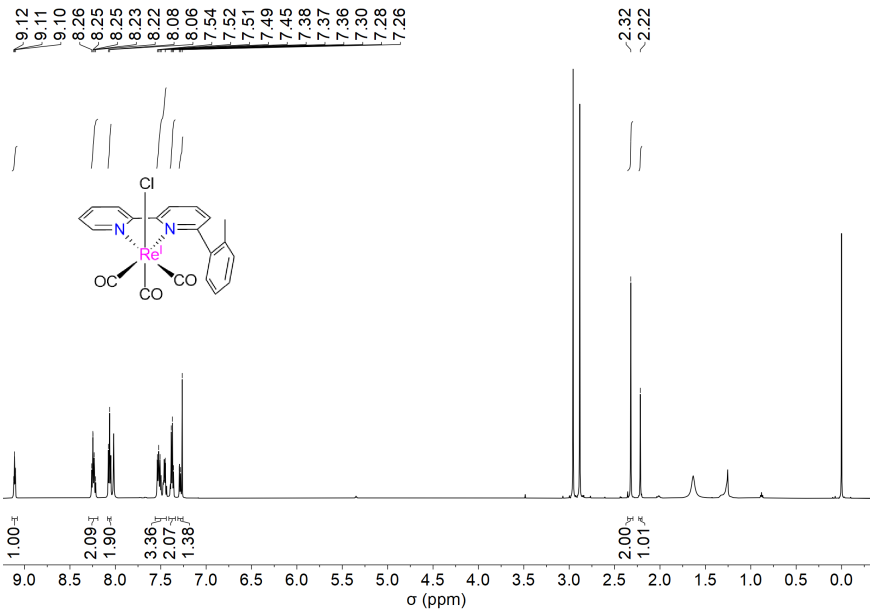

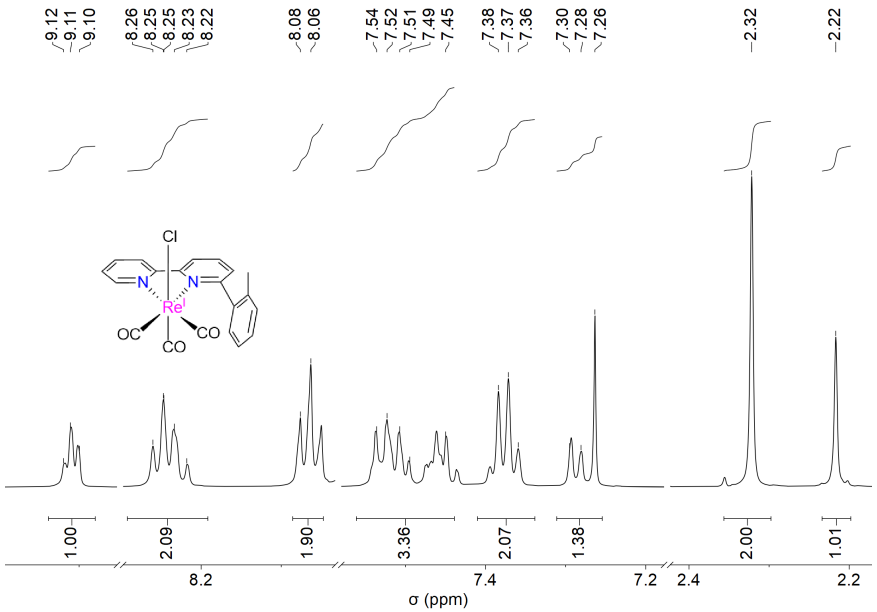

Figure S 11 ^{1}H NMR (Chloroform, 600 MHz) spectrum of **4**.

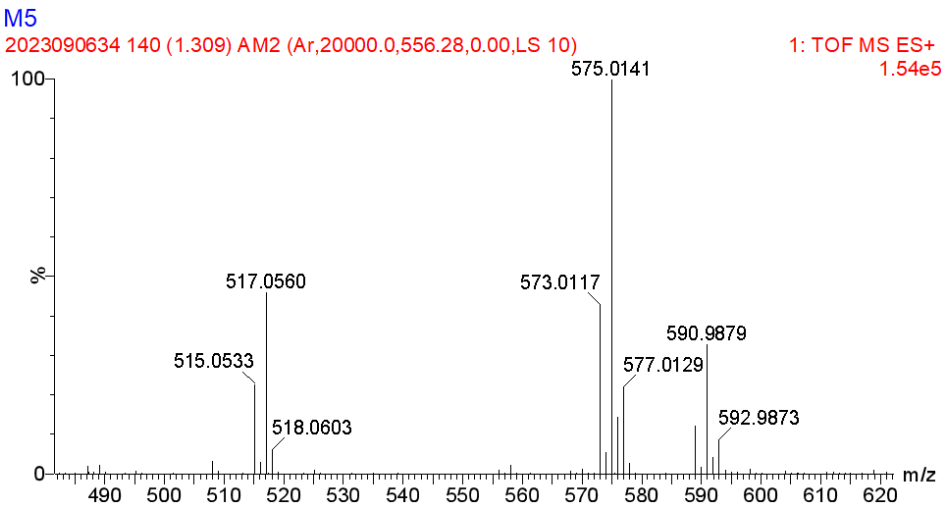

Figure S 12 high resolution mass spectrum of **4**.

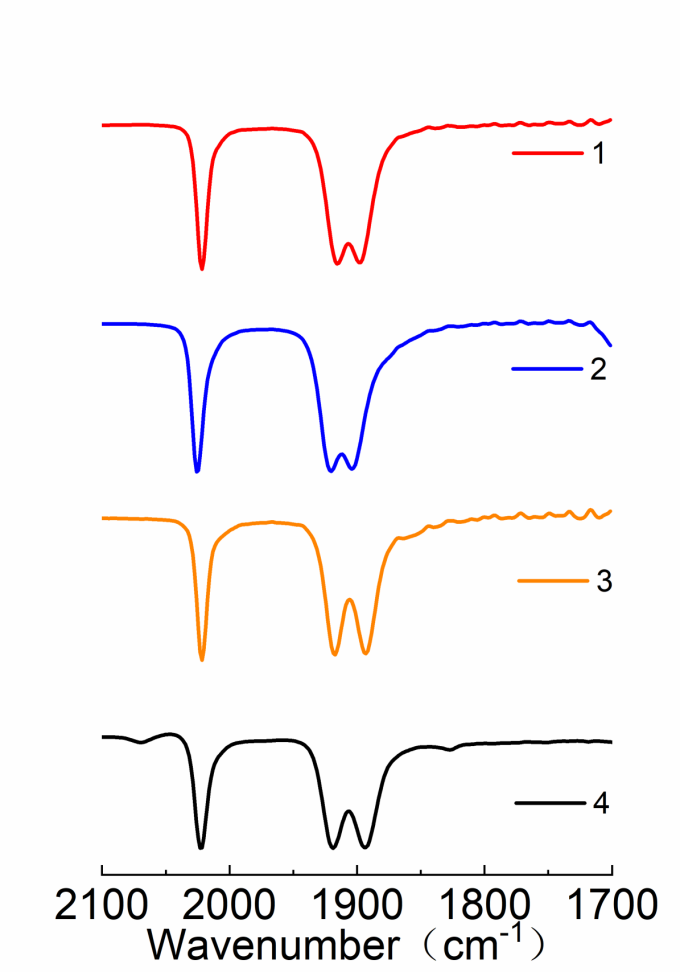

Figure S 13 Experimental FTIR spectra of **1**-**4** recorded in KBr displaying characteristic ν_{CO} stretching modes for their facial tricarbonyl geometries.

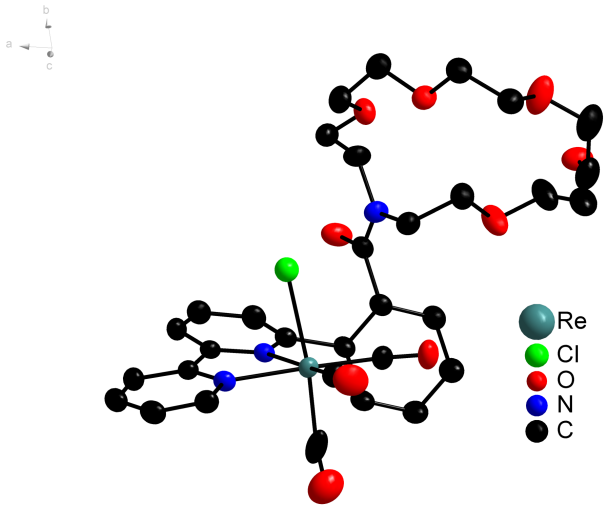

Figure S 14 Crystal structure of complex **1** with ellipsoids at 50% probability

Table S 1 Crystal data and structure refinement for **1.**

Empirical formula	$C_{32}H_{35}ClN_3O_9Re$
Formula weight	827.28
Temperature/K	220.00(10)
Crystal system	triclinic
Space group	P-1
a/Å	10.0720(2)
b/Å	10.7211(3)
c/Å	15.6647(4)
α/°	80.945(2)
β/°	80.953(2)
γ/°	75.907(2)
Volume/Å^3	1607.63(7)
Z	2
ρ_{calc}g/cm^3	1.709
μ/mm^{-1}	8.658
F(000)	824.0
Crystal size/mm^3	0.15 × 0.13 × 0.11
Radiation	Cu Kα (λ = 1.54184)
2Θ range for data collection/°	5.758 to 154.45
Index ranges	-12 ≤ h ≤ 12, -13 ≤ k ≤ 13, -19 ≤ l ≤ 19
Reflections collected	21513
Independent reflections	6472 [R_{int} = 0.0768, R_{sigma} = 0.0564]
Data/restraints/parameters	6472/355/415
Goodness-of-fit on F^2	1.088
Final R indexes [I>=2σ (I)]	R_1 = 0.0489, wR_2 = 0.1342
Final R indexes [all data]	R_1 = 0.0524, wR_2 = 0.1360

Empirical formula	$C_{32}H_{35}ClN_3O_9Re$
Largest diff. peak/hole / e $Å^{-3}$	1.08/-1.01

Table S 2 Bond Lengths for **1.**

Atom	Atom	Length/Å	Atom	Atom	Length/Å
Re1	Cl1	2.5062(15)	N3	C25	1.347(7)
Re1	N2	2.232(4)	N3	C29	1.359(7)
Re1	N3	2.167(5)	C1	C2	1.516(9)
Re1	C30	1.913(6)	C3	C4	1.500(9)
Re1	C31	1.936(5)	C5	C6	1.511(11)
Re1	C32	2.012(7)	C7	C8	1.497(12)
O1	C2	1.424(7)	C9	C10	1.505(9)
O1	C12	1.428(7)	C11	C12	1.520(9)
O2	C1	1.413(8)	C13	C14	1.505(8)
O2	C3	1.412(7)	C14	C15	1.398(8)
O3	C4	1.412(8)	C14	C19	1.416(8)
O3	C5	1.413(9)	C15	C16	1.382(9)
O4	C6	1.404(8)	C16	C17	1.402(9)
O4	C7	1.421(8)	C17	C18	1.382(9)
O5	C8	1.418(8)	C18	C19	1.404(8)
O5	C9	1.416(7)	C19	C20	1.499(8)
O6	C13	1.231(7)	C20	C21	1.392(8)
O7	C30	1.158(7)	C21	C22	1.381(9)
O8	C31	1.122(6)	C22	C23	1.381(8)
O9	C32	1.035(7)	C23	C24	1.392(7)
N1	C10	1.449(7)	C24	C25	1.482(7)
N1	C11	1.476(7)	C25	C26	1.388(8)
N1	C13	1.346(7)	C26	C27	1.381(8)
N2	C20	1.350(7)	C27	C28	1.362(9)
N2	C24	1.355(7)	C28	C29	1.379(9)

Table S 3 Bond Angles for **1.**

Atom	Atom	Atom	Angle/°	Atom	Atom	Atom	Angle/°
N2	Re1	Cl1	80.04(11)	O5	C9	C10	108.0(5)
N3	Re1	Cl1	85.45(13)	N1	C10	C9	114.2(5)
N3	Re1	N2	75.22(17)	N1	C11	C12	113.2(5)
C30	Re1	Cl1	96.37(19)	O1	C12	C11	109.1(5)
C30	Re1	N2	104.1(2)	O6	C13	N1	122.6(5)
C30	Re1	N3	178.0(2)	O6	C13	C14	118.4(5)
C30	Re1	C31	84.9(3)	N1	C13	C14	119.0(5)
C30	Re1	C32	89.0(3)	C15	C14	C13	118.5(5)
C31	Re1	Cl1	94.16(19)	C15	C14	C19	119.1(5)
C31	Re1	N2	169.7(2)	C19	C14	C13	122.0(5)
C31	Re1	N3	95.9(2)	C16	C15	C14	121.3(5)
C31	Re1	C32	91.9(3)	C15	C16	C17	119.7(6)
C32	Re1	Cl1	172.21(18)	C18	C17	C16	120.0(6)
C32	Re1	N2	93.2(2)	C17	C18	C19	120.8(5)
C32	Re1	N3	89.1(2)	C14	C19	C20	122.8(5)
C2	O1	C12	111.2(4)	C18	C19	C14	119.1(5)
C3	O2	C1	111.9(5)	C18	C19	C20	117.8(5)
C4	O3	C5	114.3(6)	N2	C20	C19	119.4(5)
C6	O4	C7	113.9(6)	N2	C20	C21	121.4(5)
C9	O5	C8	114.9(5)	C21	C20	C19	119.0(5)
C10	N1	C11	117.0(4)	C22	C21	C20	120.2(5)
C13	N1	C10	125.8(5)	C21	C22	C23	118.5(5)
C13	N1	C11	117.3(5)	C22	C23	C24	119.3(5)
C20	N2	Re1	126.9(4)	N2	C24	C23	122.2(5)
C20	N2	C24	118.4(4)	N2	C24	C25	116.5(4)
C24	N2	Re1	113.5(3)	C23	C24	C25	121.3(5)
C25	N3	Re1	117.0(3)	N3	C25	C24	115.9(5)
C25	N3	C29	118.4(5)	N3	C25	C26	121.1(5)
C29	N3	Re1	124.6(4)	C26	C25	C24	123.0(5)
O2	C1	C2	109.5(5)	C27	C26	C25	119.9(6)
O1	C2	C1	109.3(5)	C28	C27	C26	119.1(5)
O2	C3	C4	110.3(5)	C27	C28	C29	119.2(5)
O3	C4	C3	107.2(5)	N3	C29	C28	122.2(6)
O3	C5	C6	112.7(6)	O7	C30	Re1	175.0(5)
O4	C6	C5	107.7(6)	O8	C31	Re1	179.7(7)
O4	C7	C8	110.1(7)	O9	C32	Re1	172.9(7)
O5	C8	C7	112.9(7)				

9. Detail discussions on the IR-SEC of complexes

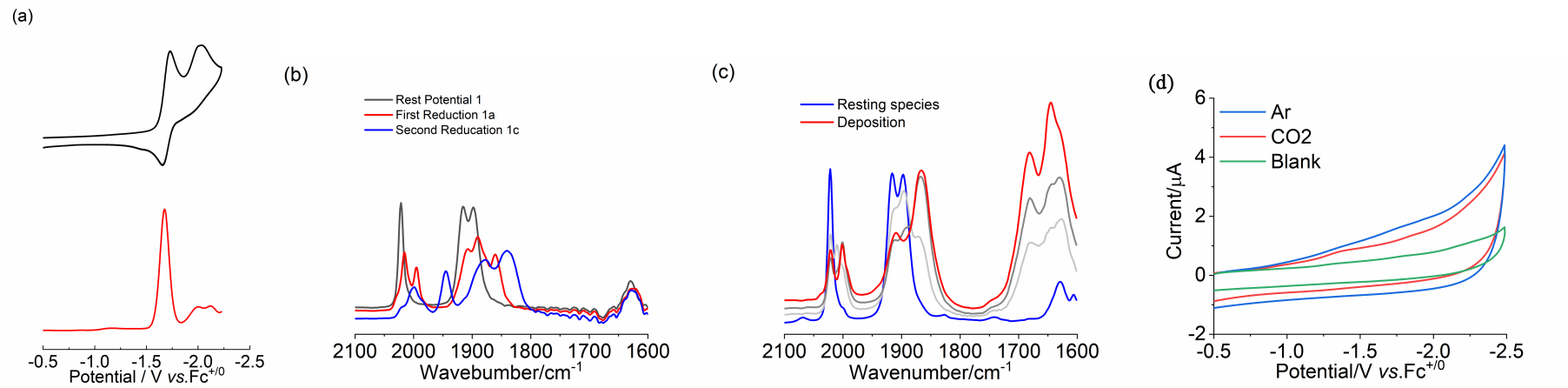

Figure S 15 (a) CV and DPV of complex **1** (0.5 mM) in acetonitrile under Ar. (b) IR-SEC of 3 mM precursor **1** (black, 2022 1916 and 1897 cm^{-1}) under an atmosphere of Ar in MeCN with 25mM KPF_6 and 0.1 M $^nBu_4NPF_6$ as the supporting electrolyte, showing two major species as the potential is increased cathodically: **$(Re^I(bpy^{\bullet-})(CO)_3)Cl$** coordination model (red, 1997 1890 and 1861 cm^{-1}), the doubly reduced species **$(Re^0(bpy^{\bullet-})(CO)_3)$** (blue, 1946 and 1841 cm^{-1}). (c) IR-SEC of 3 mM **1** at -1.9 V under CO_2 in the presence of 25 mM KPF_6 in acetonitrile with 0.1 M $^nBu_4NPF_6$ electrolyte. The resting species (blue, **1**) has three ν_{CO} stretches at 2023, 1924, and 1897 cm^{-1}. When the voltage of the cell is held at approximately -1.9 V for more than 1 min, the deposition (red) formed with four ν_{CO} stretches at 2000, 1866, 1681 and 1645 cm^{-1}. (d) CVs of 25 mM KPF_6 under Ar (blue line) and CO_2 (red line).

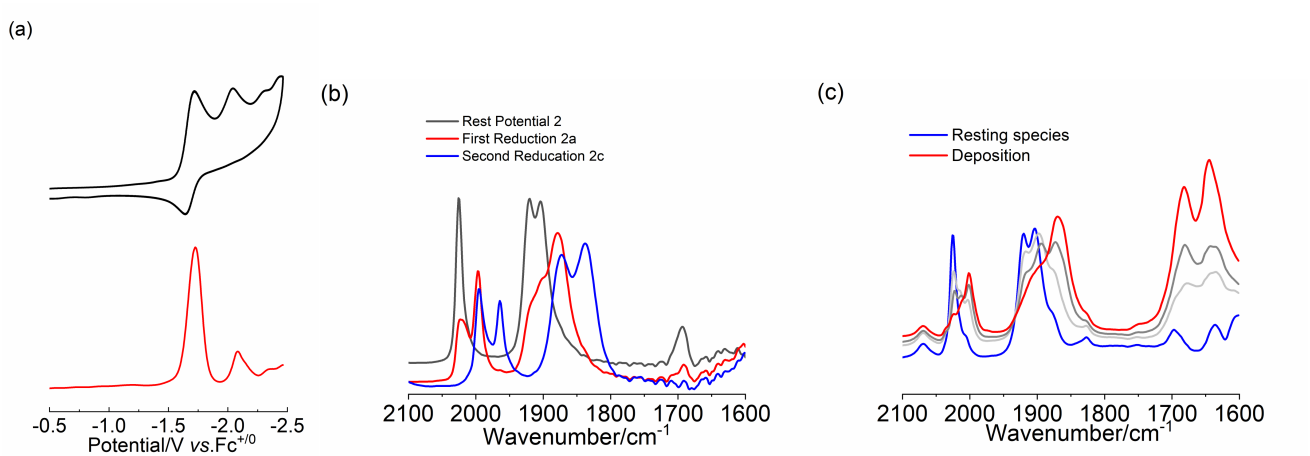

Figure S 16 (a) CV and DPV of complex **2** (0.5 mM) in acetonitrile under Ar. (b) IR-SEC of 3 mM precursor **2** (black, 2025 1920 and 1904 cm^{-1}) under an atmosphere of Ar in MeCN with 25mM KPF_6 and 0.1 M $^{n}Bu_4NPF_6$ as the supporting electrolyte, showing two major species as the potential is increased cathodically: **$(Re^{I}(bpy^{\bullet-})(CO)_3)Cl$** coordination model (red, 1997 1902 and 1880 cm^{-1}), the doubly reduced species **$(Re^{0}(bpy^{\bullet-})(CO)_3)$** (blue, 1964 and 1839 cm^{-1}). (c) IR-SEC of 3 mM **2** at -1.9 V under CO_2 in the presence of 25 mM KPF_6 in acetonitrile with 0.1 M $^{n}Bu_4NPF_6$ electrolyte. The resting species (blue, **2**) has three ν_{CO} stretches at 2026, 1920, and 1904 cm^{-1}. When the voltage of the cell is held at approximately -1.9 V for more than 1 min, the deposition (red) formed with four ν_{CO} stretches at 2001, 1870, 1682 and 1644 cm^{-1}.

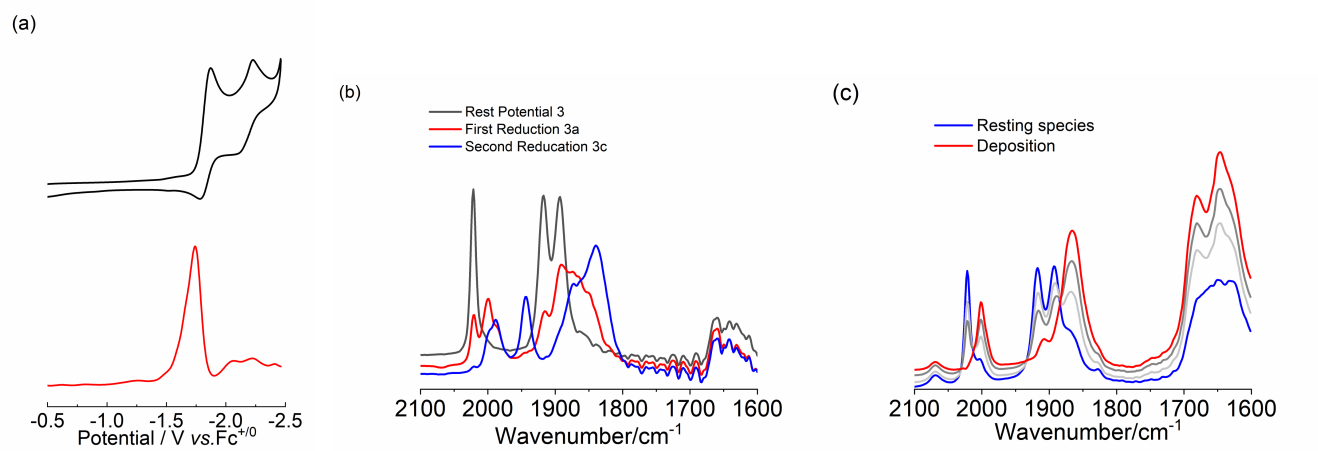

Figure S 17 (a) CV and DPV of complex **3** (0.5 mM) in acetonitrile under Ar. (b) IR-SEC of 3 mM precursor **3** (black, 2022 1917 and 1893 cm^{-1}) under an atmosphere of Ar in MeCN with 25mM KPF_6 and 0.1 M $^{n}Bu_4NPF_6$ as the supporting electrolyte, showing two major species as the potential is increased cathodically: **$(Re^{I}(bpy^{\bullet-})(CO)_3)Cl$** coordination model (red, 2000 1874 and 1866 cm^{-1}), the doubly reduced species **$(Re^{0}(bpy^{\bullet-})(CO)_3)$** (blue, 1944 and 1840 cm^{-1}). (c) IR-SEC of 3 mM **3** at -1.9 V under CO_2 in the presence of 25 mM KPF_6 in acetonitrile with 0.1 M $^{n}Bu_4NPF_6$ electrolyte. The resting species (blue, **3**) has three ν_{CO} stretches at 2022, 1917, and 1893 cm^{-1}. When the voltage of the cell is held at approximately -1.9 V for more than 1 min, the deposition (red) formed with four ν_{CO} stretches at 2002, 1866, 1681 and 1647 cm^{-1}.

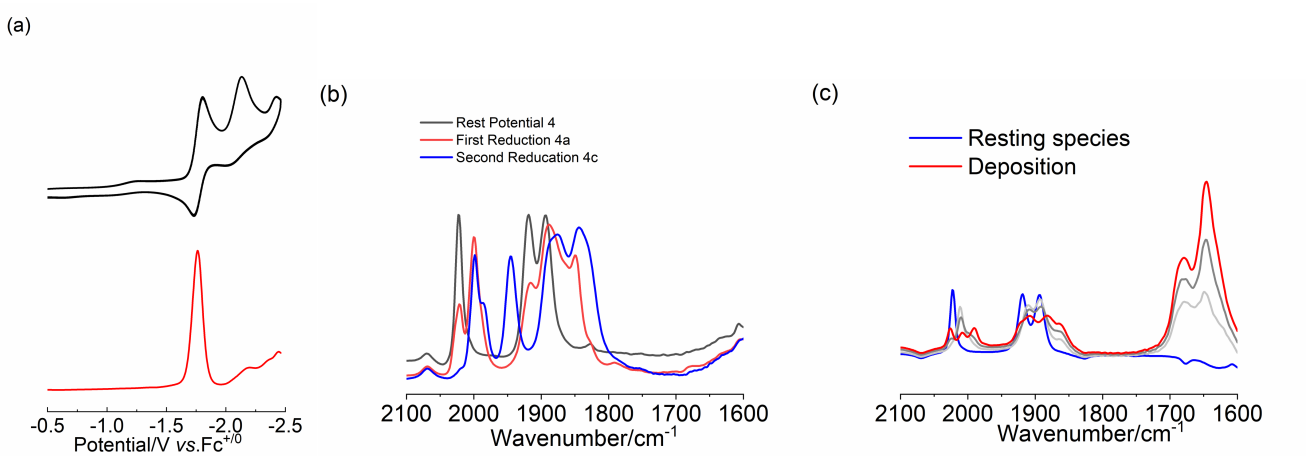

Figure S 18 (a) CV and DPV of complex **4** (0.5 mM) in acetonitrile under Ar. (b) IR-SEC of 3 mM precursor **4** (black, 2022 1918 and 1893 cm^{-1}) under an atmosphere of Ar in MeCN with 25mM KPF_6 and 0.1 M $^{n}Bu_4NPF_6$ as the supporting electrolyte, showing two major species as the potential is increased cathodically: **$(Re^{I}(bpy^{\bullet-})(CO)_3)Cl$** coordination model (red, 2000 1888 and 1850 cm^{-1}), the doubly reduced species **$(Re^{0}(bpy^{\bullet-})(CO)_3)$** (blue, 1946 and 1844 cm^{-1}). (c) IR-SEC of 3 mM **4** at -1.9 V under CO_2 in the presence of 25 mM KPF_6 in acetonitrile with 0.1 M $^{n}Bu_4NPF_6$ electrolyte. The resting species (blue, **4**) has three ν_{CO} stretches at 2023, 1920, and 1894 cm^{-1}. When the voltage of the cell is held at approximately -1.9 V for more than 1 min, the deposition (red) formed with four ν_{CO} stretches at 1990, 1862, 1679 and 1645 cm^{-1}.

Table S 4 The absorption peaks for the complexes **1-4**, and their corresponding mono-reduced species and doubly reduced species in the presence of 25 mM KPF_6 in acetonitrile solution. The data for the absorption peaks were obtained from the IR-SEC test. The control test was taken under the same condition with complex **4** in the absence of crown and KPF_6.

Complex (3 mM)	Intrinsic peak (cm^{-1})	the mono- reduced species (cm^{-1})	the doubly reduced species (cm^{-1})
1	2022、1916、1897	1997、1890、1861	1946、1841
2	2025、1920、1904	1997、1902、1880	1964、1839
3	2022、1917、1893	2000、1874、1866	1944、1840
4	2022、1918、1893	2000、1888、1850	1946、1844
4	2021、1918、1892	1999、1879、1849	1946、1843

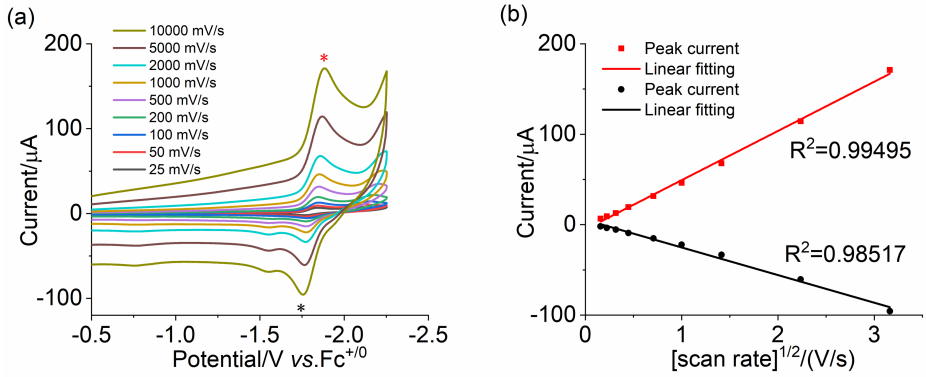

Figure S 19 (a) CVs of complex **1** (0.5 mM) with scan rate (v) varied from 0.025 V/s to 10 V/s under Ar; (b) Plot of redox peak current (i_p) *vs.* $v^{1/2}$ for complex **1**. Voltammograms are taken with 0.1 M ^{n}Bu$_4$NPF$_6$ in MeCN solution. Glassy carbon working electrode, Ag$^+$/Ag reference electrode, and Pt wire counter electrode.

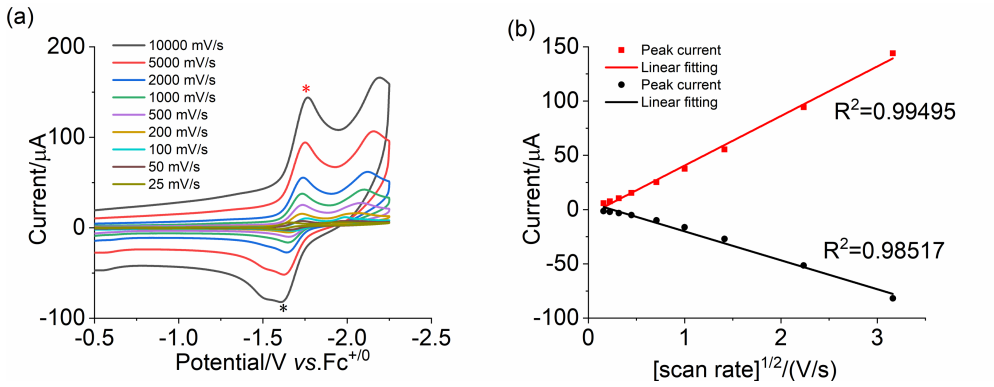

Figure S 20 (a) CVs of complex **2** (0.5 mM) with scan rate (v) varied from 0.025 V/s to 10 V/s under Ar; (b) Plot of redox peak current (i_p) *vs.* $v^{1/2}$ for complex **2**. Voltammograms are taken with 0.1 M ^{n}Bu$_4$NPF$_6$ in MeCN solution. Glassy carbon working electrode, Ag$^+$/Ag reference electrode, and Pt wire counter electrode.

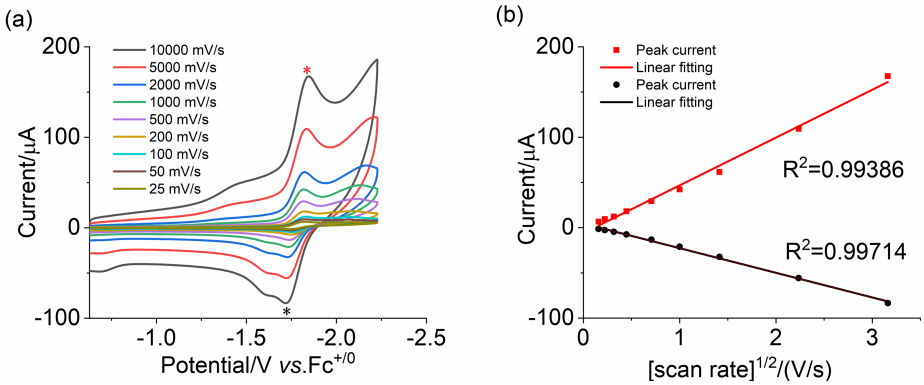

Figure S 21 (a) CVs of complex **3** (0.5 mM) with scan rate (v) varied from 0.025 V/s to 10 V/s under Ar; (b) Plot of redox peak current (i_p) *vs.* $v^{1/2}$ for complex **3**. Voltammograms are taken with 0.1 M $^{n}Bu_4NPF_6$ in MeCN solution. Glassy carbon working electrode, Ag^{+}/Ag reference electrode, and Pt wire counter electrode.

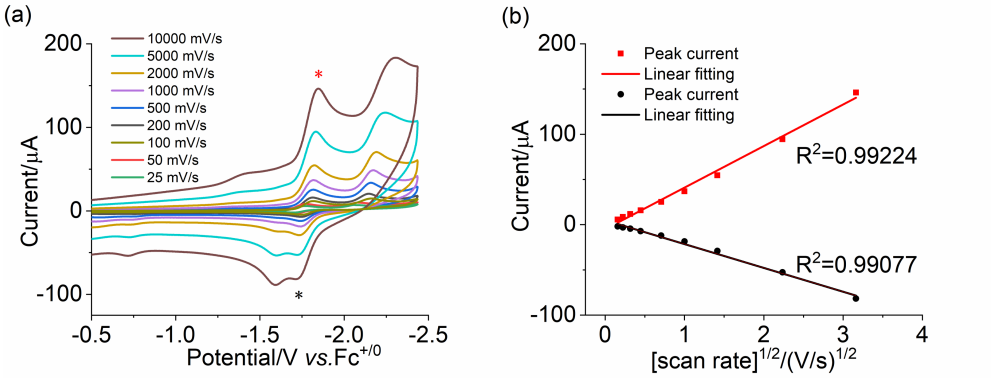

Figure S 22 (a) CVs of complex **4** (0.5 mM) with scan rate (v) varied from 0.025 V/s to 10 V/s under Ar; (b) Plot of redox peak current (i_p) *vs.* $v^{1/2}$ for complex **4**. Voltammograms are taken with 0.1 M $^{n}Bu_4NPF_6$ in MeCN solution. Glassy carbon working electrode, Ag^{+}/Ag reference electrode, and Pt wire counter electrode.

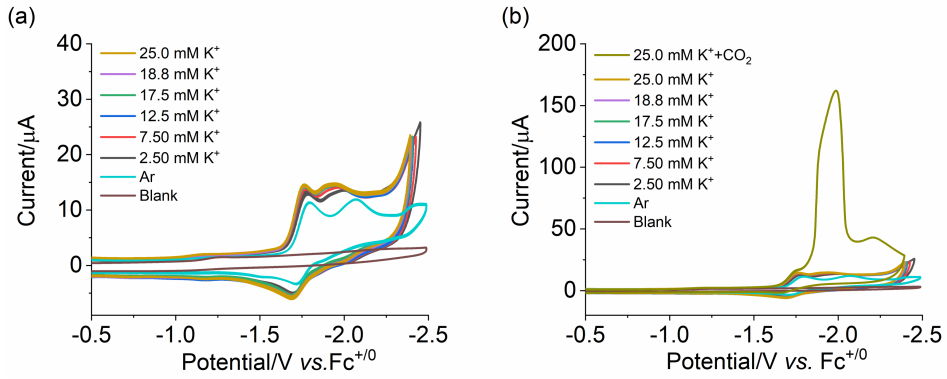

Figure S 23 (a) CVs of 0.5 mM **1** with varied concentrations of KPF_6 under Ar. (b) CVs show 0.5 mM **1** with varied amounts of KPF_6 under Ar, and saturated with CO_2 in the presence of 25 mM KPF_6. Voltammograms are taken at a scan rate of 100 mV/s with 0.1 M $^nBu_4NPF_6$ in MeCN solution. Glassy carbon working electrode, Ag^+/Ag reference electrode, and Pt wire counter electrode.

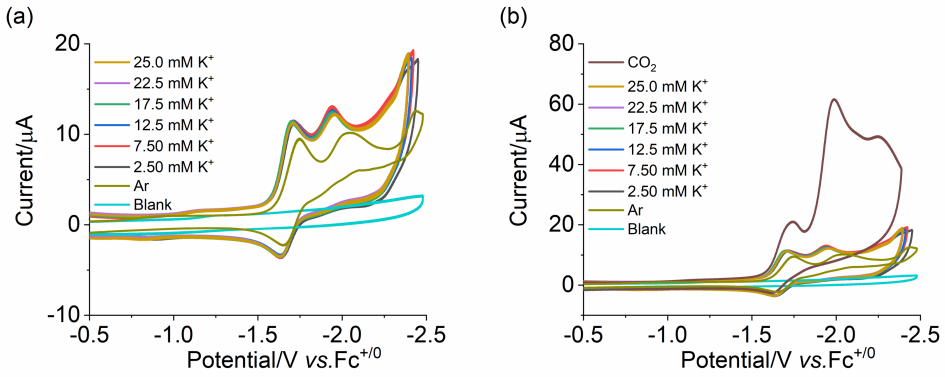

Figure S 24 (a) CVs of 0.5 mM **2** with varied concentrations of KPF_6 under Ar. (b) CVs show 0.5 mM **2** with varied amounts of KPF_6 under Ar, and saturated with CO_2 in the presence of 25 mM KPF_6. Voltammograms are taken at a scan rate of 100 mV/s with 0.1 M $^nBu_4NPF_6$ in MeCN solution. Glassy carbon working electrode, Ag^+/Ag reference electrode, and Pt wire counter electrode.

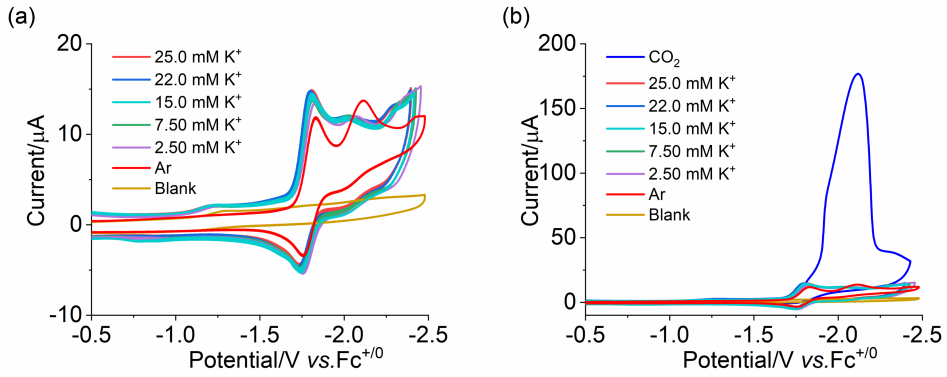

Figure S 25 (a) CVs of 0.5 mM **3** with varied concentrations of KPF_6 under Ar. (b) CVs show 0.5 mM **3** with varied amounts of KPF_6 under Ar, and saturated with CO_2 in the presence of 25 mM KPF_6. Voltammograms are taken at a scan rate of 100 mV/s with 0.1 M $^nBu_4NPF_6$ in MeCN solution. Glassy carbon working electrode, Ag^+/Ag reference electrode, and Pt wire counter electrode.

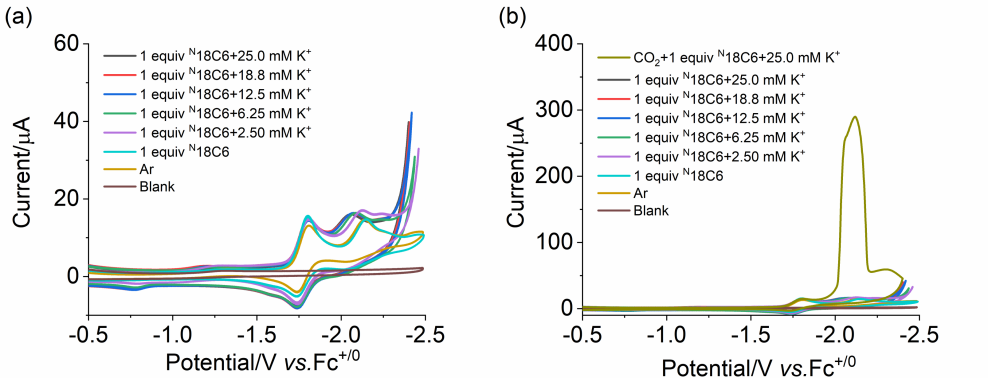

Figure S 26 (a) CVs of 0.5 mM **4** with varied concentrations of KPF_6 under Ar. (b) CVs show 0.5 mM **4** with varied amounts of KPF_6 under Ar, and saturated with CO_2 in the presence of 25 mM KPF_6. Voltammograms are taken at a scan rate of 100 mV/s with 0.1 M $^nBu_4NPF_6$ in MeCN solution. Glassy carbon working electrode, Ag^+/Ag reference electrode, and Pt wire counter electrode.

10. Determinantion of the equilibrium binding constant of K_{K^+}

According to the modified Nernst equation (1), as the concentration of K^+ dissolved in solution varied, a gradually increasing positive shift in potential followed the increasing K^+ concentration. A plot of $E_{1/2}$ *vs.* ln [K^+] was found to be linear (Figure S 27), suggesting that the modified Nernst equation (1) is applicable for the case. The second redox event for the complexes **1**-**4** in our manuscript are all irreversible. In operation, we use the half-peak potentials ($E^{p/2}$) for representing $E^{1/2}$ (H. G. Roth, N. A. Romero, and D. A. Nicewicz, *Synlett*, 2016, **27**, 714). E^0 is the formal potential for doubly reduced intermediate ($Re^0(bpy^{\bullet-})(CO)_3$) in the absence of binding, and $\boldsymbol{q}$ is the number of K^+ involved in the binding. The slope obtained from these results was 0.026 V/decade. This value is consistent with the binding of a single K^+ to the crown. The intercept was used to obtain an equilibrium binding constant of K_{K^+}. The equilibrium binding constant of K_{K^+} for complexes **1**-**4** were summarized in table S 4. The equilibrium binding constant of K_{K^+} for complex **2** is *ca.* two orders larger than that for another three, which is consistent with the alkalinity of the amine in the crown. In addition, the equilibrium binding constant of K_{K^+} for complexes **1** and **3** are close to that for the complex **4** with a separated crown, implying a weaker binding effect for complexes **1** and **3**.

$$E_{1/2} = E^0 + (RT/nF)\ln K_{[K^+]} + q(RT/nF)\ln [K^+] \quad (1)$$

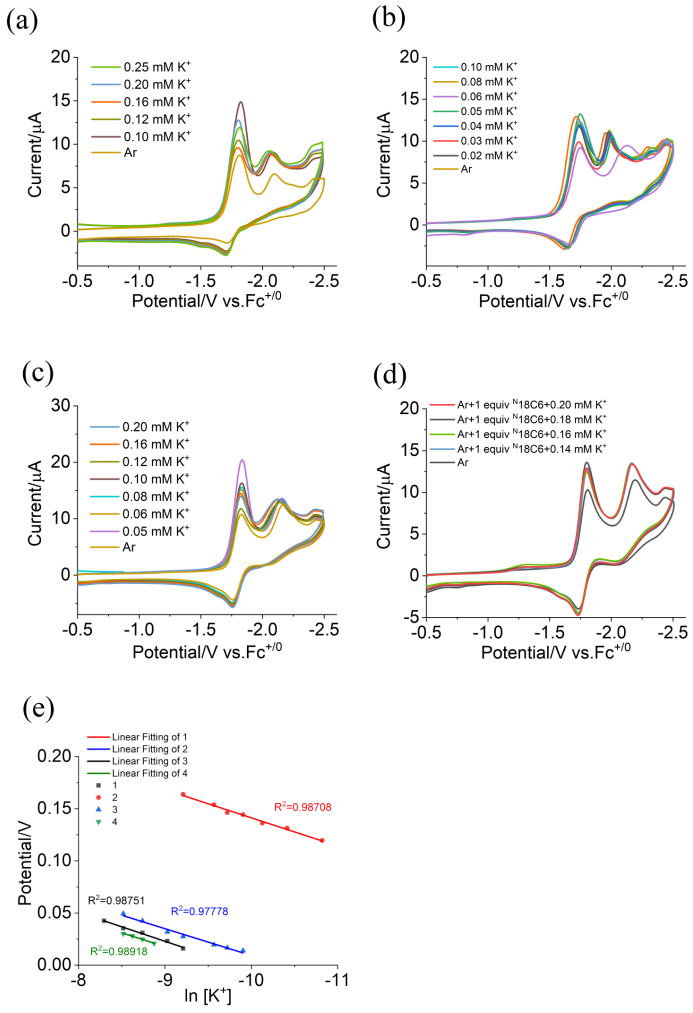

Figure S 27 (a) CVs show 0.5 mM **1** with varied concentrations of KPF_6 under Ar. (b) CVs show 0.5 mM **2** with varied concentrations of KPF_6 under Ar. (c) CVs show 0.5 mM **3** with varied concentrations of KPF_6 under Ar. (d) CVs show 0.5 mM **4** with varied concentrations of KPF_6 under Ar. (e) Plot of potential difference *vs.* ln [K^+] for complex **1**-**4.** Voltammograms are taken at a scan rate of 100 mV/s with 0.1 M ^{n}Bu$_4$NPF$_6$ in MeCN solution. Glassy carbon working electrode, Ag^+/Ag reference electrode, and Pt wire counter electrode.

Table S 5 The equilibrium binding constant of K_{K^+} for complexes **1**-**4**

Complex (0.5 mM)	**1**	**2**	**3**	**4**
Binding constant of K_{K^+}	3.7×10^4	7.5×10^6	2.8×10^4	1.7×10^4

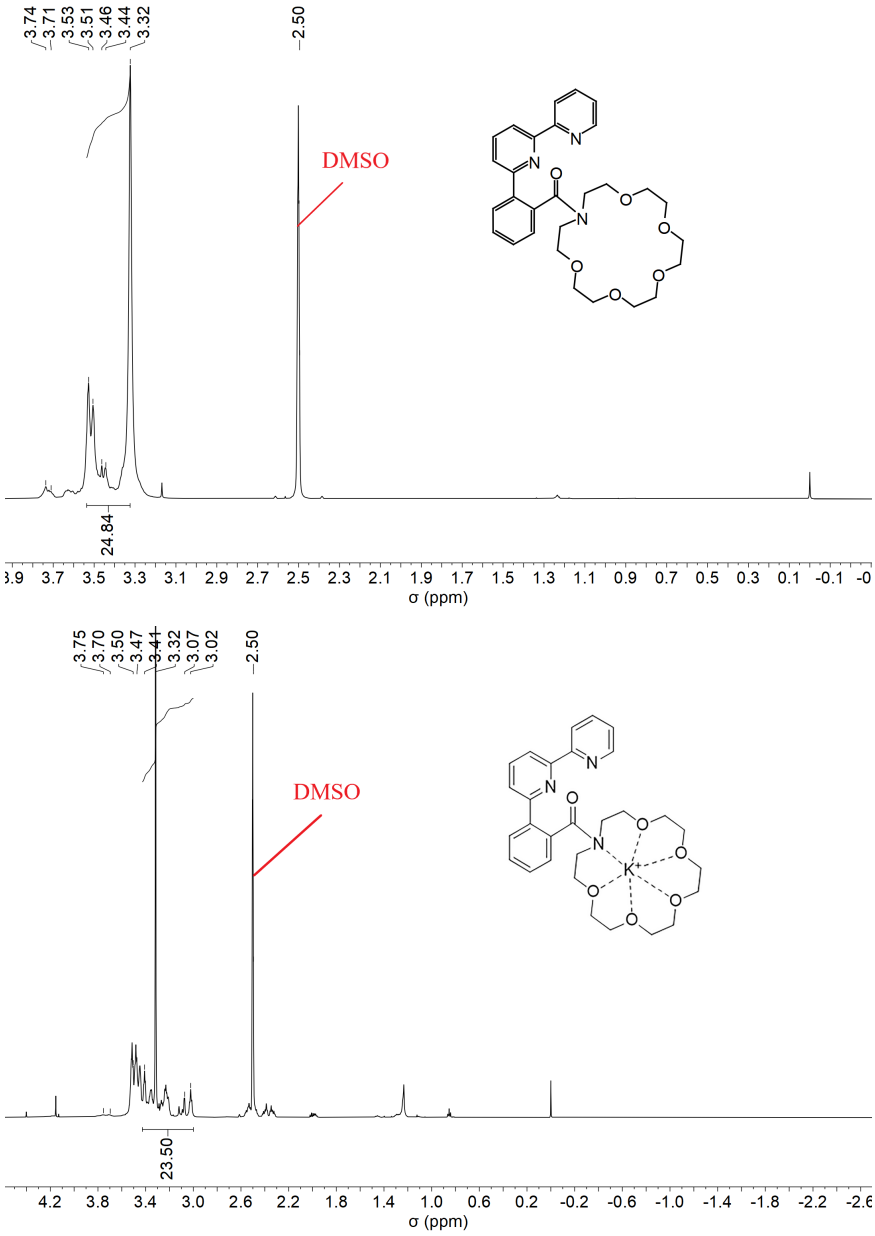

Figure S 28 (a) ^{1}H NMR (DMSO, 600 MHz) spectrum of $\mathbf{L_1}$ (up). (b) ^{1}H NMR (DMSO, 600 MHz) spectrum of $\mathbf{L_1}$ with K^+ (down).

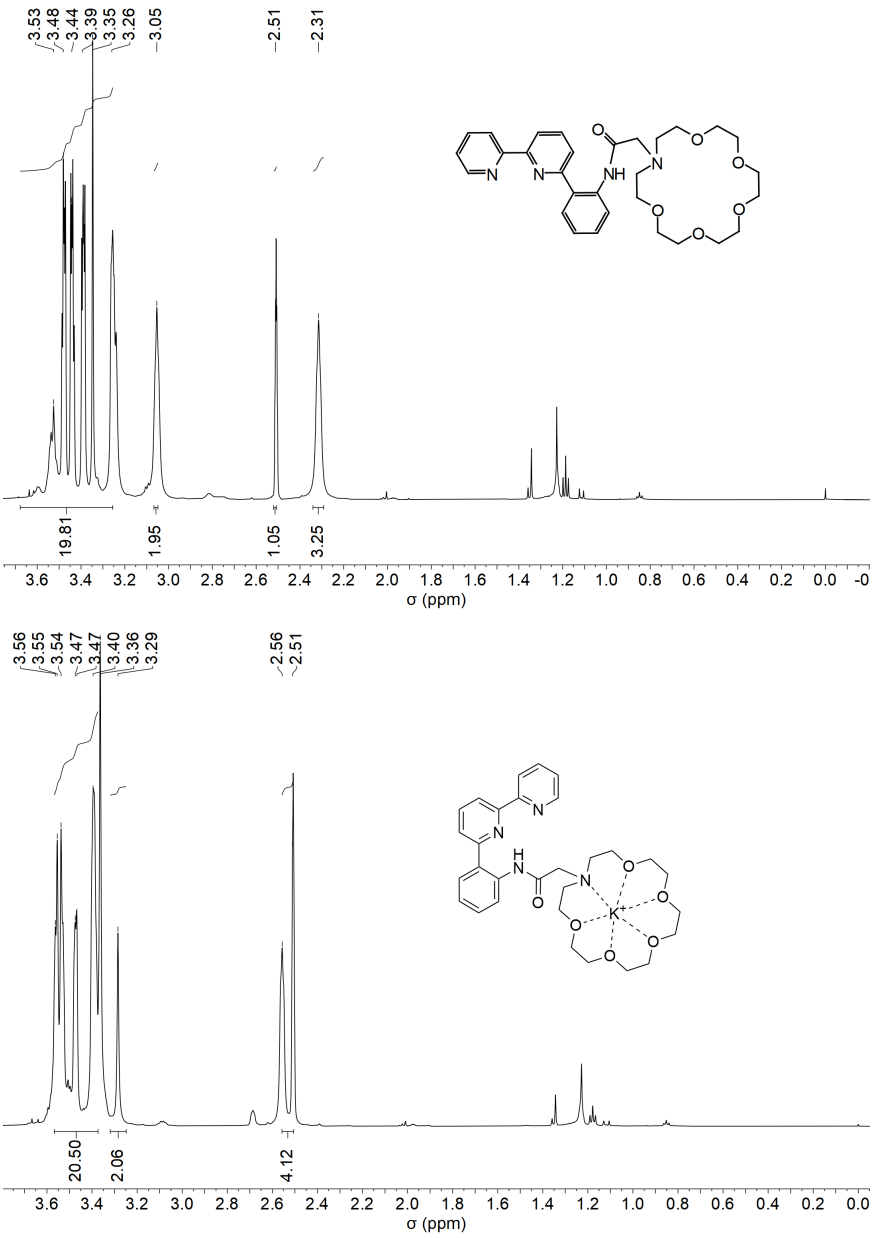

Figure S 29 (a) ^{1}H NMR (DMSO, 600 MHz) spectrum of $\mathbf{L_2}$ (up). (b) ^{1}H NMR (DMSO, 600 MHz) spectrum of $\mathbf{L_2}$ with K^+ (down).

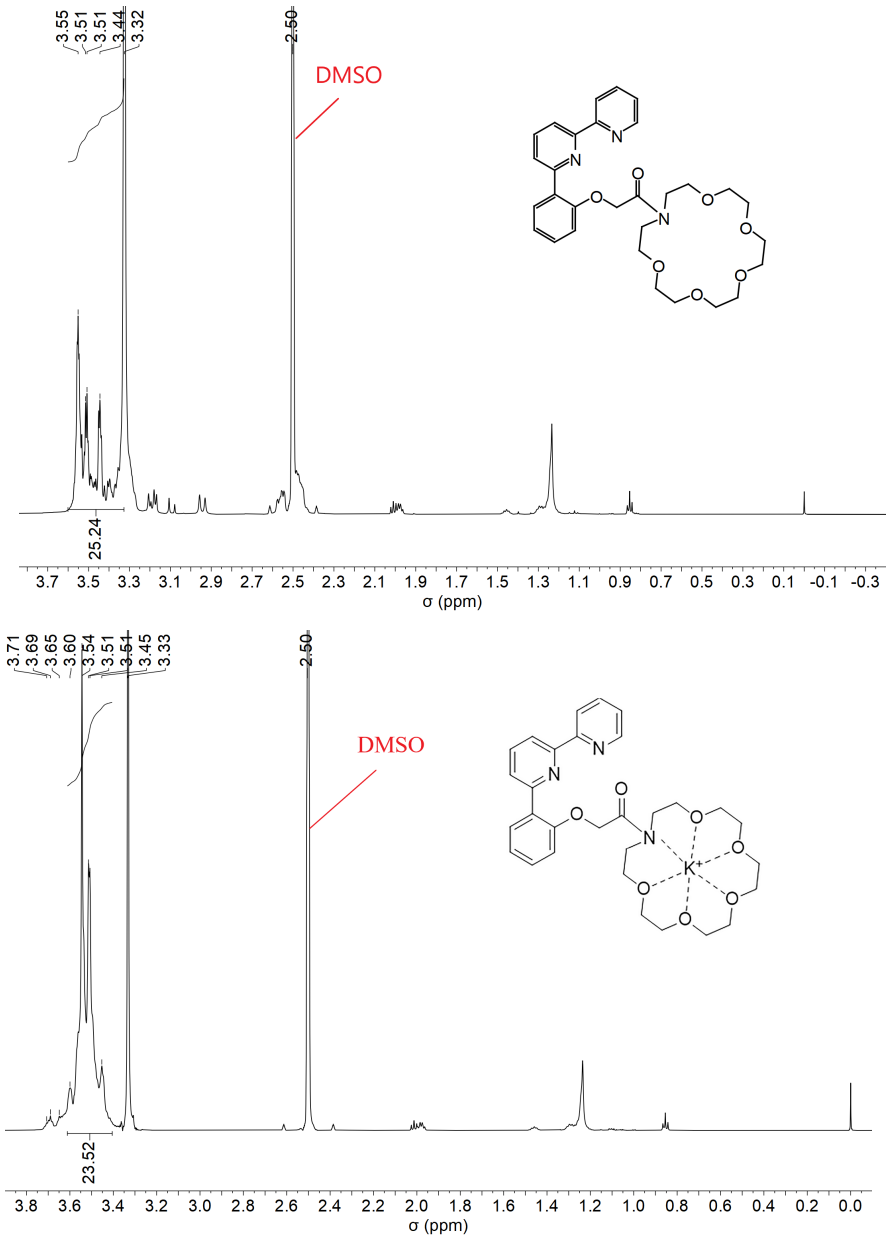

Figure S 30 (a) ^{1}H NMR (DMSO, 600 MHz) spectrum of $\mathbf{L_3}$ (up). (b) ^{1}H NMR (DMSO, 600 MHz) spectrum of $\mathbf{L_3}$ with K^+ (down).

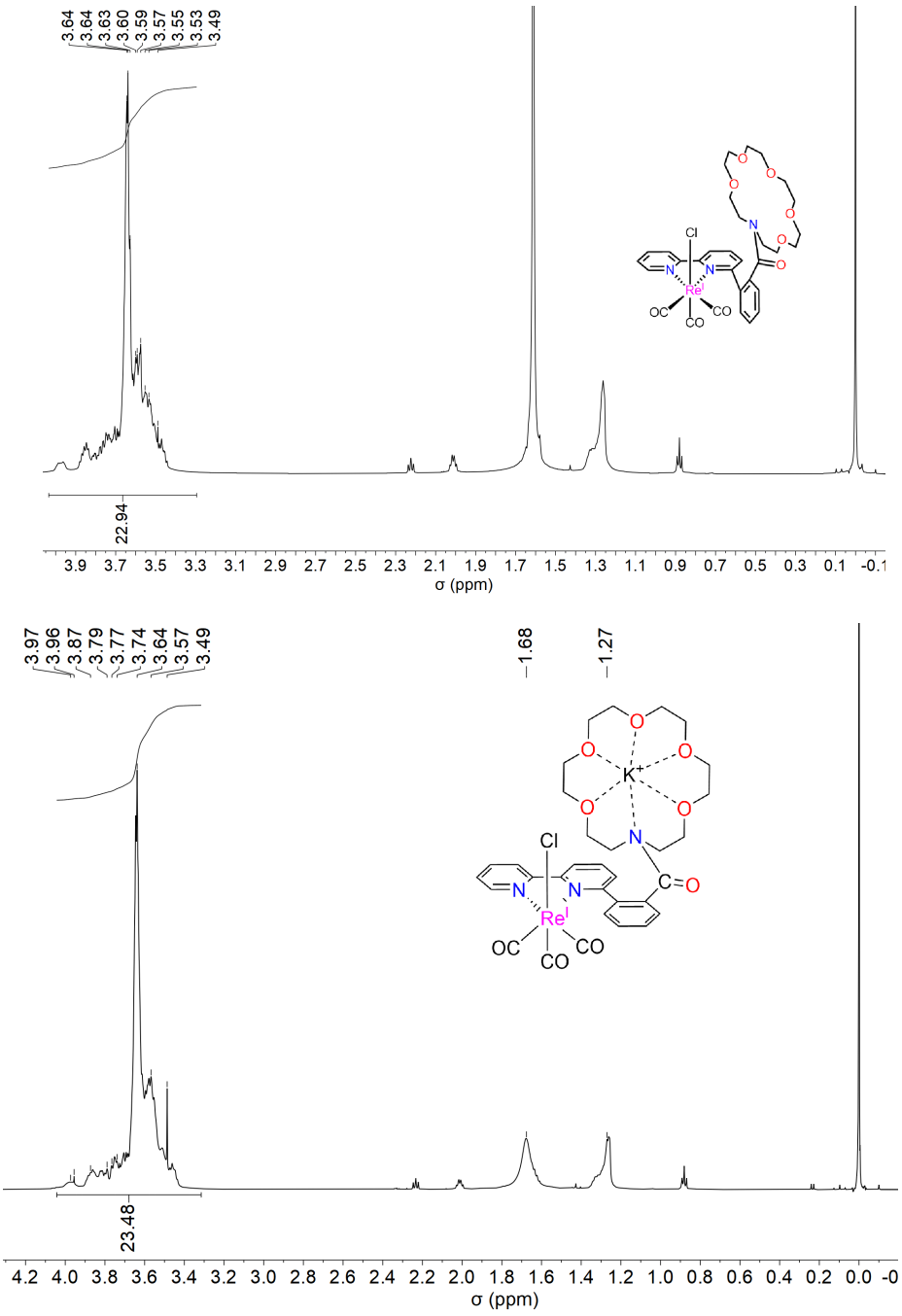

Figure S 31(a) ^{1}H NMR (Chloroform, 600 MHz) spectrum of **1** (up). (b) ^{1}H NMR (Chloroform, 600 MHz) spectrum of **1** with K^{+} (down).

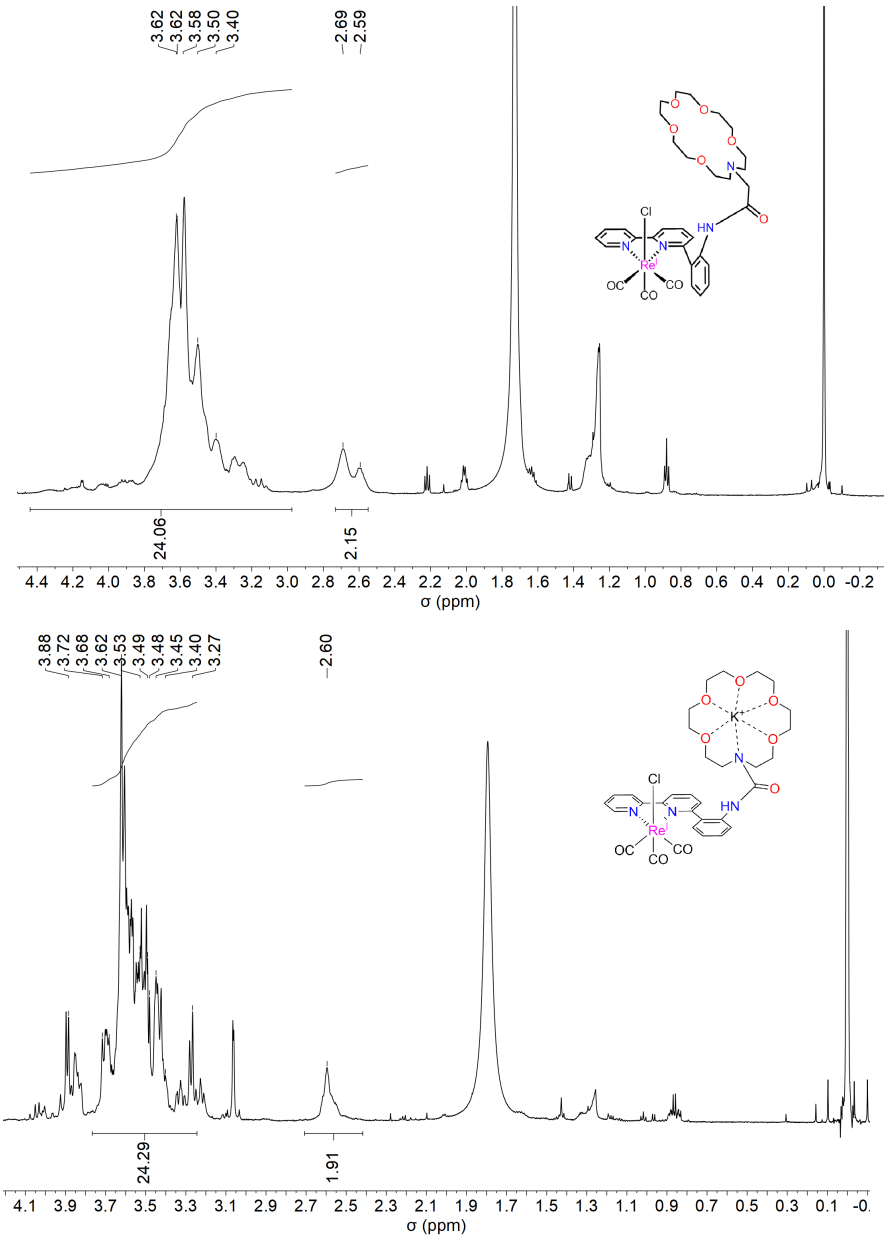

Figure S 32 (a) ^{1}H NMR (Chloroform, 600 MHz) spectrum of **2** (up). (b) ^{1}H NMR (Chloroform, 600 MHz) spectrum of **2** with K^{+} (down).

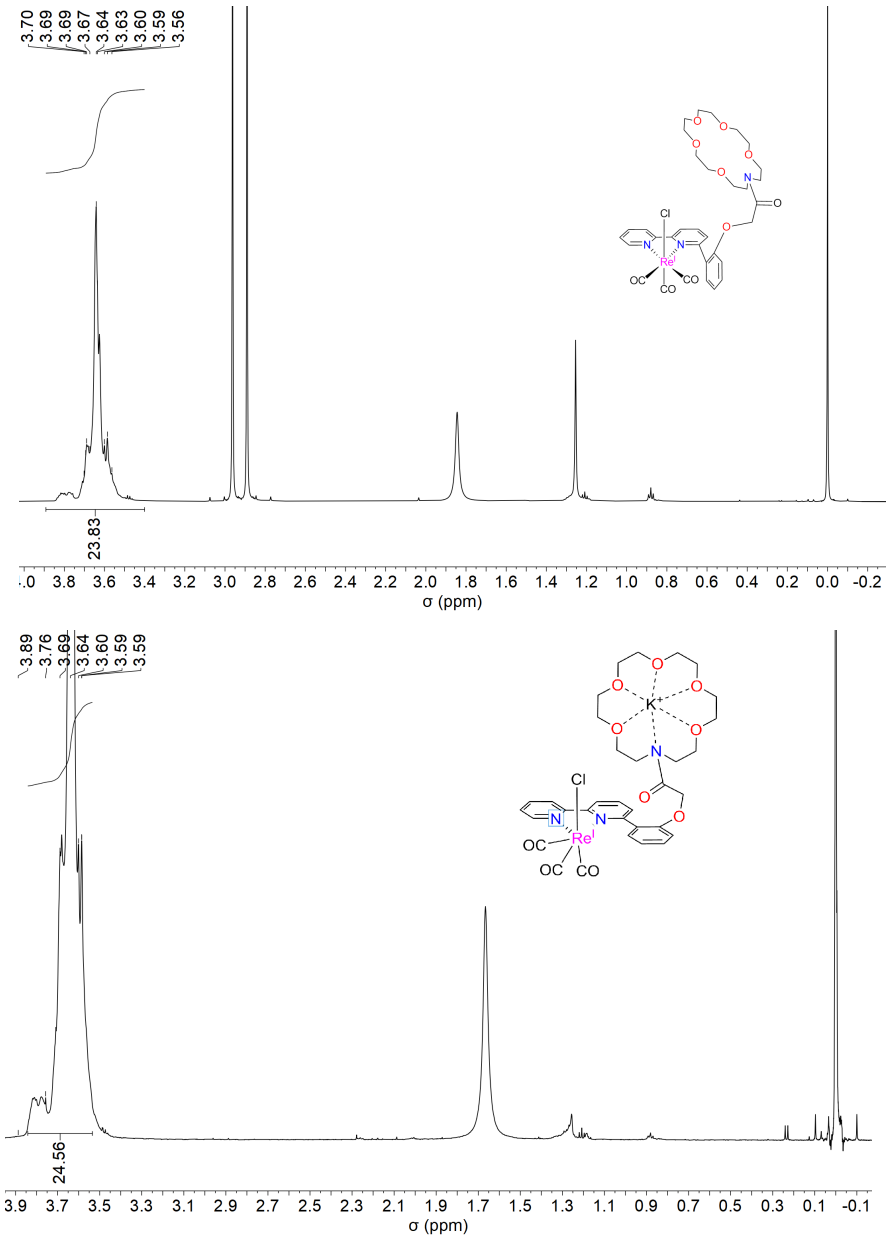

Figure S 33 (a) ^{1}H NMR (Chloroform, 600 MHz) spectrum of **3** (up). (b) ^{1}H NMR (Chloroform, 600 MHz) spectrum of **3** with K^{+} (down).

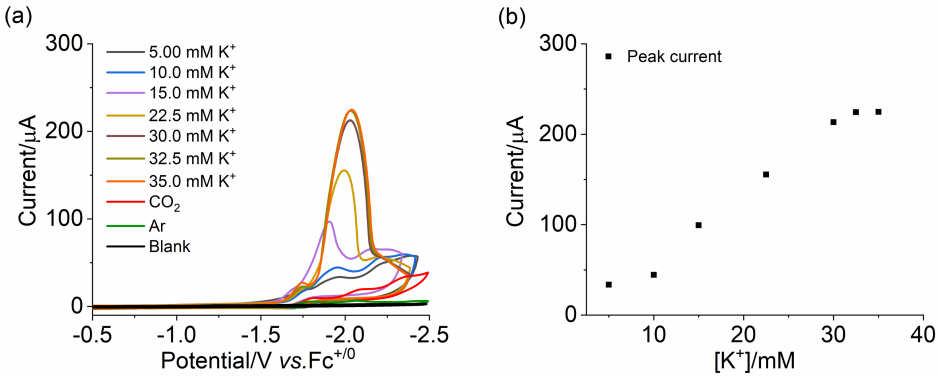

Figure S 34 (a) CVs show 0.5 mM **1** with varied amounts of KPF_6 under CO_2. (b) The dependence of peak point current (i_{cat}) on the concentration of KPF_6. Voltammograms are taken at a scan rate of 100 mV/s with 0.1 M $^{n}Bu_4NPF_6$ in MeCN solution. Glassy carbon working electrode, Ag^{+}/Ag reference electrode, and Pt wire counter electrode.

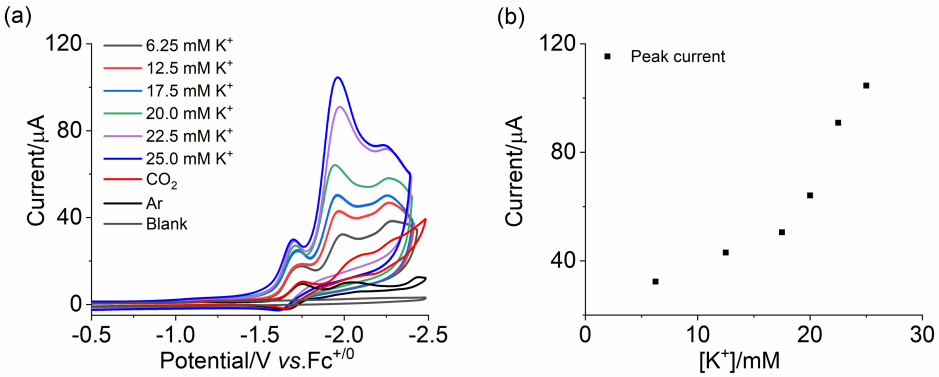

Figure S 35 (a) CVs show 0.5 mM **2** with varied amounts of KPF_6 under CO_2. (b) The dependence of peak point current (i_{cat}) on the concentration of KPF_6. Voltammograms are taken at a scan rate of 100 mV/s with 0.1 M $^{n}Bu_4NPF_6$ in MeCN solution. Glassy carbon working electrode, Ag^{+}/Ag reference electrode, and Pt wire counter electrode.

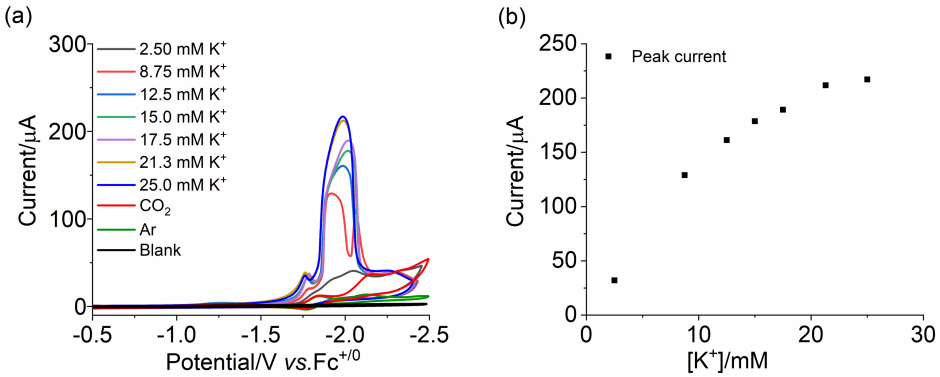

Figure S 36 (a) CVs show 0.5 mM **3** with varied amounts of KPF_6 under CO_2. (b) The dependence of peak point current (i_{cat}) on the concentration of KPF_6. Voltammograms are taken at a scan rate of 100 mV/s with 0.1 M $^{n}Bu_4NPF_6$ in MeCN solution. Glassy carbon working electrode, Ag^{+}/Ag reference electrode, and Pt wire counter electrode.

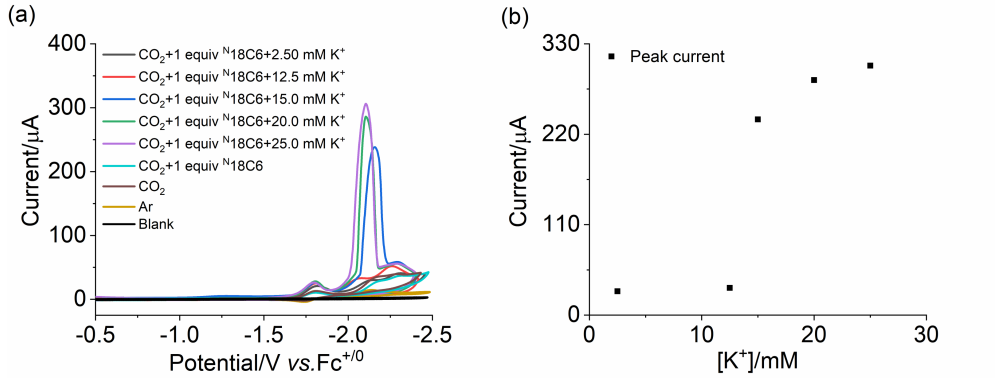

Figure S 37 (a) CVs show 0.5 mM **4** with varied amounts of KPF_6 under CO_2. (b) The dependence of peak point current(i_{cat}) on the concentration of KPF_6. Voltammograms are taken at a scan rate of 100 mV/s with 0.1 M $^{n}Bu_4NPF_6$ in MeCN solution. Glassy carbon working electrode, Ag^{+}/Ag reference electrode, and Pt wire counter electrode.

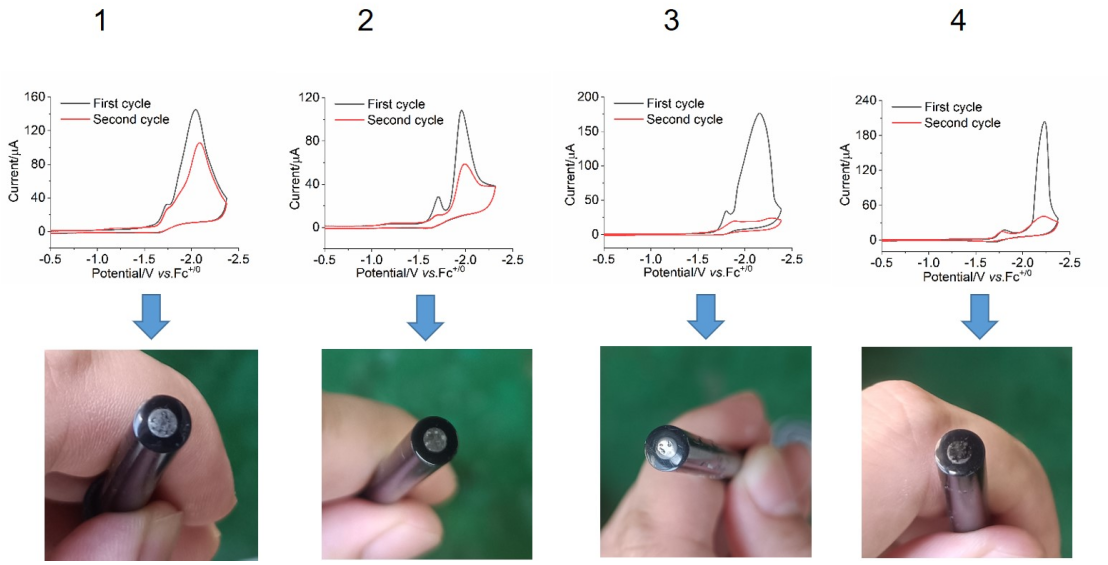

Figure S 38 The first and the second cycle of the CVs of 0.5 mM **1**-**4** in the presence of 25 mM KPF_6 under CO_2 (up). (b) the photographs of the electrode after two scan cycles (down). Voltammograms are taken at a scan rate of 100 mV/s with 0.1 M $^{n}Bu_4NPF_6$ in MeCN solution. Glassy carbon working electrode, Ag^{+}/Ag reference electrode, and Pt wire counter electrode.

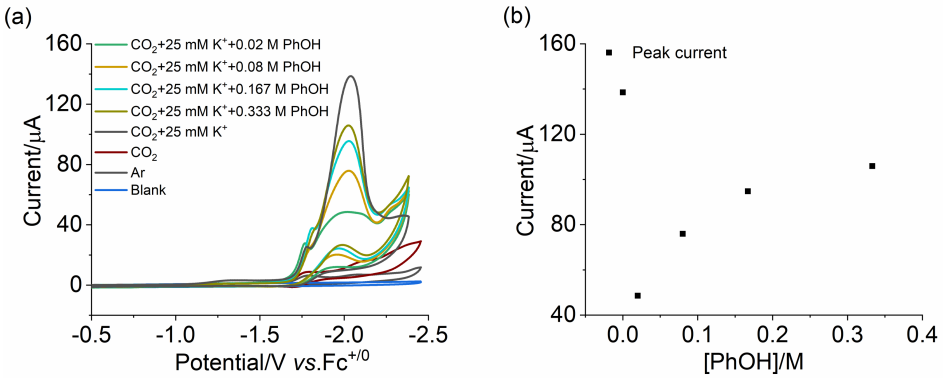

Figure S 39 (a) CVs show 0.5 mM **1** and 25 mM KPF_6 with varied amounts of PhOH under CO_2. (b) Plot of peak current *vs.* varied amounts of PhOH for complex **1**. Voltammograms are taken at a scan rate of 100 mV/s with 0.1 M $^{n}Bu_4NPF_6$ in MeCN solution. Glassy carbon working electrode, Ag^{+}/Ag reference electrode, and Pt wire counter electrode.

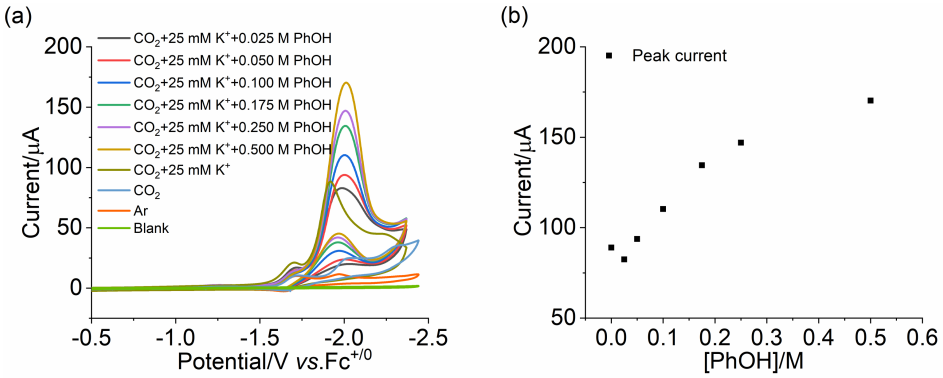

Figure S 40 (a) CVs show 0.5 mM **2** and 25 mM KPF_6 with varied amounts of PhOH under CO_2. (b) Plot of peak current *vs.* varied amounts of PhOH for complex **2**. Voltammograms are taken at a scan rate of 100 mV/s with 0.1 M $^{n}Bu_4NPF_6$ in MeCN solution. Glassy carbon working electrode, Ag^{+}/Ag reference electrode, and Pt wire counter electrode.

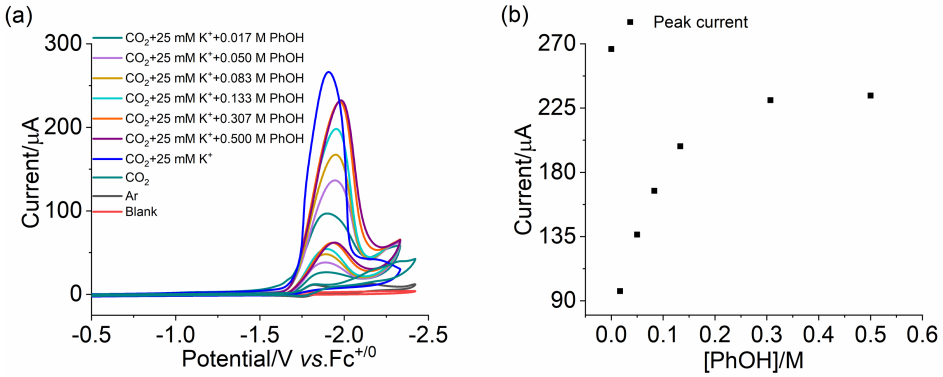

Figure S 41 (a) CVs show 0.5 mM **3** and 25 mM KPF_6 with varied amounts of PhOH under CO_2. (b) Plot of peak current *vs.* varied amounts of PhOH for complex **3**. Voltammograms are taken at a scan rate of 100 mV/s with 0.1 M $^nBu_4NPF_6$ in MeCN solution. Glassy carbon working electrode, Ag^+/Ag reference electrode, and Pt wire counter electrode.

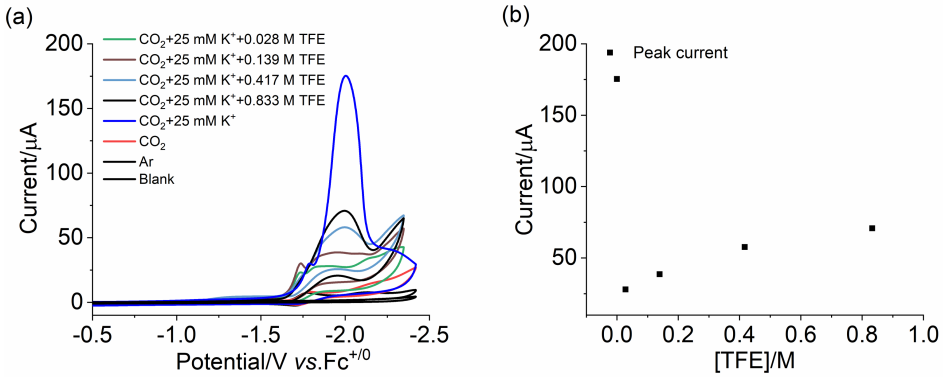

Figure S 42 (a) CVs show 0.5 mM **1** and 25 mM KPF_6 with varied amounts of TFE under CO_2. (b) Plot of peak current *vs.* varied amounts of TFE for complex **1**. Voltammograms are taken at a scan rate of 100 mV/s with 0.1 M $^{n}Bu_4NPF_6$ in MeCN solution. Glassy carbon working electrode, Ag^{+}/Ag reference electrode, and Pt wire counter electrode.

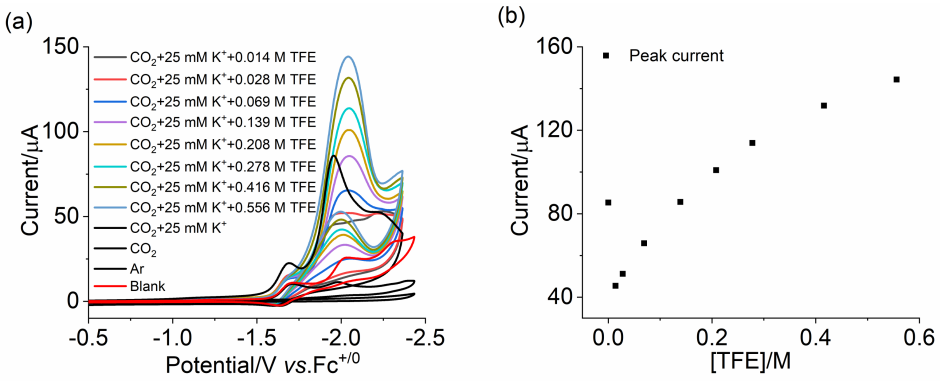

Figure S 43 (a) CVs show 0.5 mM **2** and 25 mM KPF_6 with varied amounts of TFE under CO_2. (b) Plot of peak current *vs.* varied amounts of TFE for complex **2**. Voltammograms are taken at a scan rate of 100 mV/s with 0.1 M $^{n}Bu_4NPF_6$ in MeCN solution. Glassy carbon working electrode, Ag^{+}/Ag reference electrode, and Pt wire counter electrode.

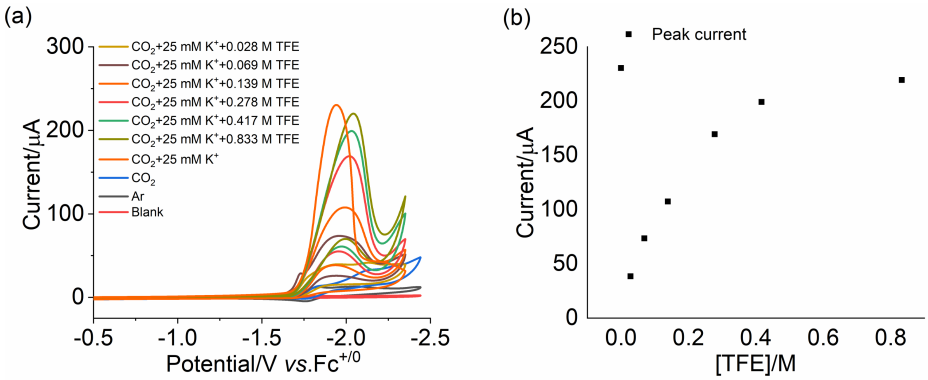

Figure S 44 (a) CVs show 0.5 mM **3** and 25 mM KPF_6 with varied amounts of TFE under CO_2. (b) Plot of peak current *vs.* varied amounts of TFE for complex **3**. Voltammograms are taken at a scan rate of 100 mV/s with 0.1 M $^{n}Bu_4NPF_6$ in MeCN solution. Glassy carbon working electrode, Ag^{+}/Ag reference electrode, and Pt wire counter electrode.

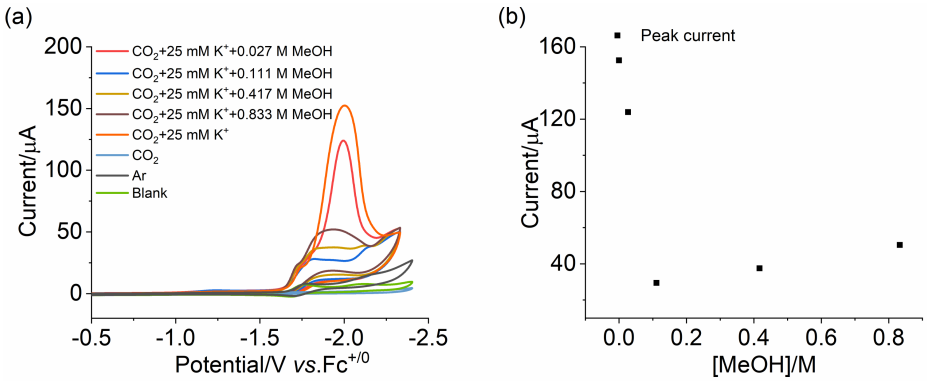

Figure S 45 (a) CVs show 0.5 mM **1** and 25 mM KPF_6 with varied amounts of MeOH under CO_2. (b) Plot of peak current *vs.* varied amounts of MeOH for complex **1**. Voltammograms are taken at a scan rate of 100 mV/s with 0.1 M $^{n}Bu_4NPF_6$ in MeCN solution. Glassy carbon working electrode, Ag^{+}/Ag reference electrode, and Pt wire counter electrode.

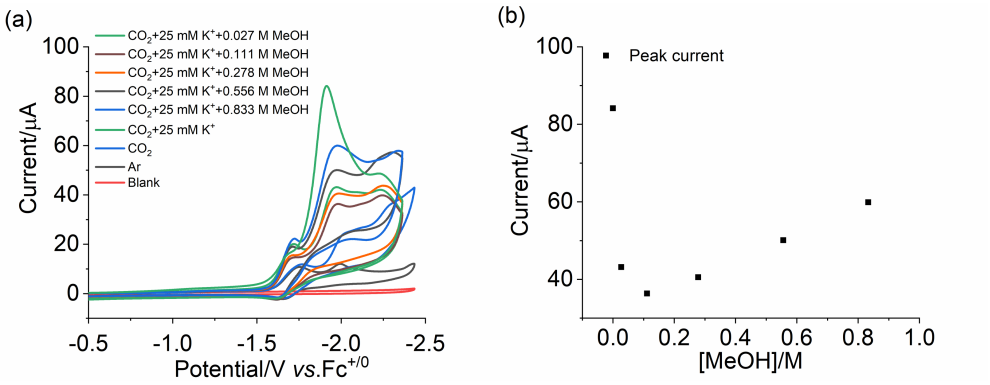

Figure S 46 (a) CVs show 0.5 mM **2** and 25 mM KPF_6 with varied amounts of MeOH under CO_2. (b) Plot of peak current *vs.* varied amounts of MeOH for complex **2**. Voltammograms are taken at a scan rate of 100 mV/s with 0.1 M $^nBu_4NPF_6$ in MeCN solution. Glassy carbon working electrode, Ag^+/Ag reference electrode, and Pt wire counter electrode.

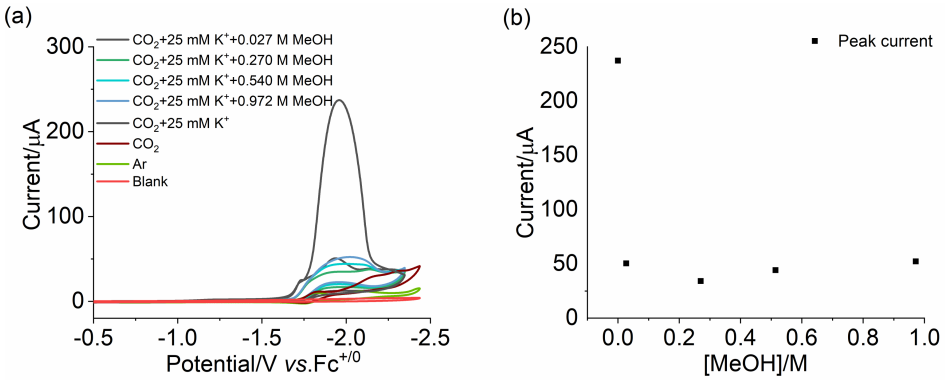

Figure S 47 (a) CVs show 0.5 mM **3** and 25 mM KPF_6 with varied amounts of MeOH under CO_2. (b) Plot of peak current *vs.* varied amounts of MeOH for complex **3**. Voltammograms are taken at a scan rate of 100 mV/s with 0.1 M $^{n}Bu_4NPF_6$ in MeCN solution. Glassy carbon working electrode, Ag^{+}/Ag reference electrode, and Pt wire counter electrode.

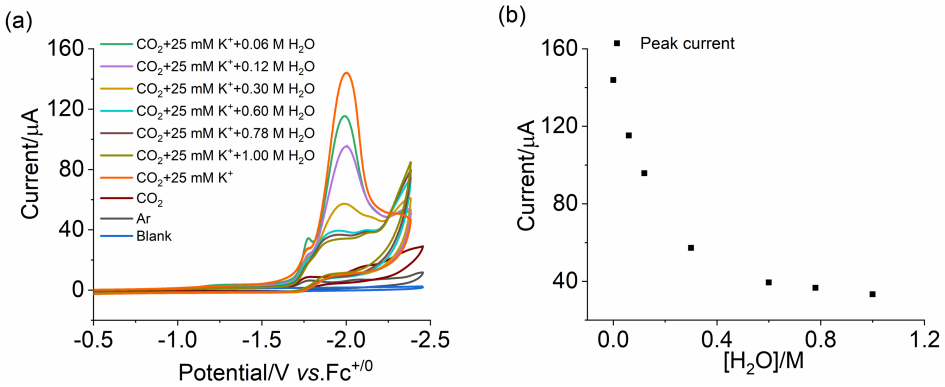

Figure S 48 (a) CVs show 0.5 mM **1** and 25 mM KPF_6 with varied amounts of H_2O under CO_2. (b) Plot of peak current *vs.* varied amounts of H_2O for complex **1**. Voltammograms are taken at a scan rate of 100 mV/s with 0.1 M $^{n}Bu_4NPF_6$ in MeCN solution. Glassy carbon working electrode, Ag^{+}/Ag reference electrode, and Pt wire counter electrode.

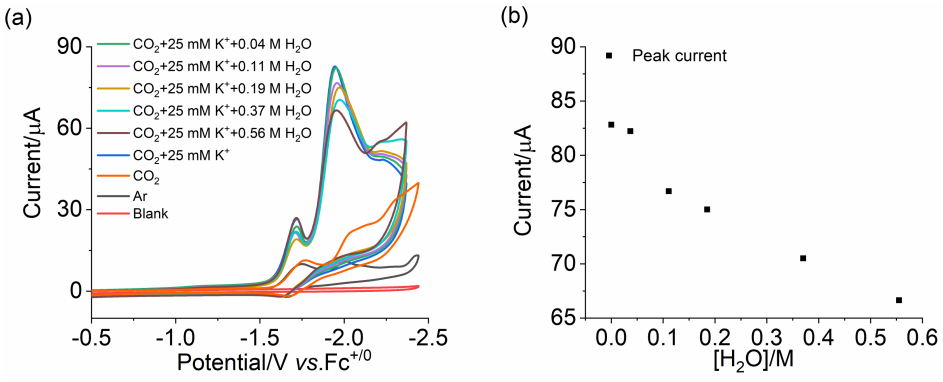

Figure S 49 (a) CVs show 0.5 mM **2** and 25 mM KPF_6 with varied amounts of H_2O under CO_2. (b) Plot of peak current *vs.* varied amounts of H_2O for complex **2**. Voltammograms are taken at a scan rate of 100 mV/s with 0.1 M $^{n}Bu_4NPF_6$ in MeCN solution. Glassy carbon working electrode, Ag^{+}/Ag reference electrode, and Pt wire counter electrode.

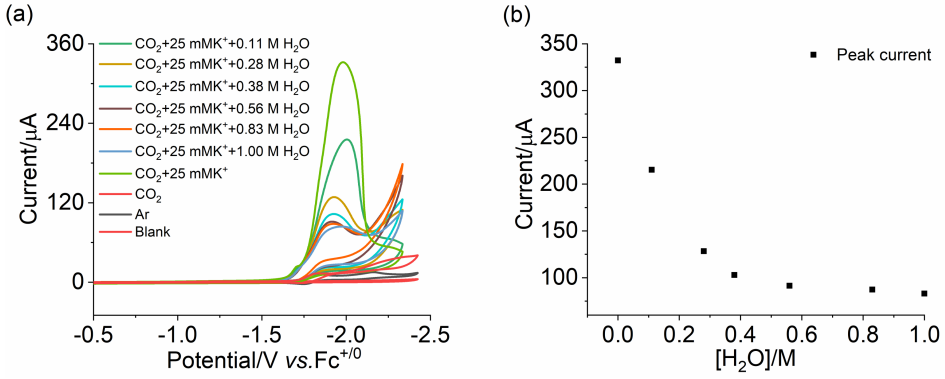

Figure S 50 (a) CVs show 0.5 mM **3** and 25 mM KPF_6 with varied amounts of H_2O under CO_2. (b) Plot of peak current *vs.* varied amounts of H_2O for complex **3**. Voltammograms are taken at a scan rate of 100 mV/s with 0.1 M $^{n}Bu_4NPF_6$ in MeCN solution. Glassy carbon working electrode, Ag^{+}/Ag reference electrode, and Pt wire counter electrode.

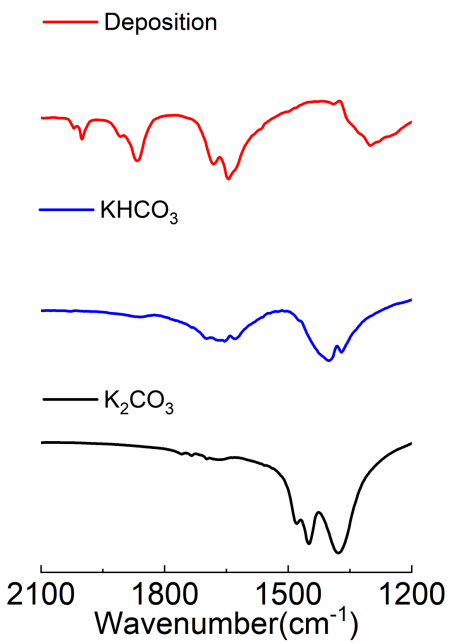

Figure S 51 IR-SEC of Deposition $KHCO_3$ and K_2CO_3

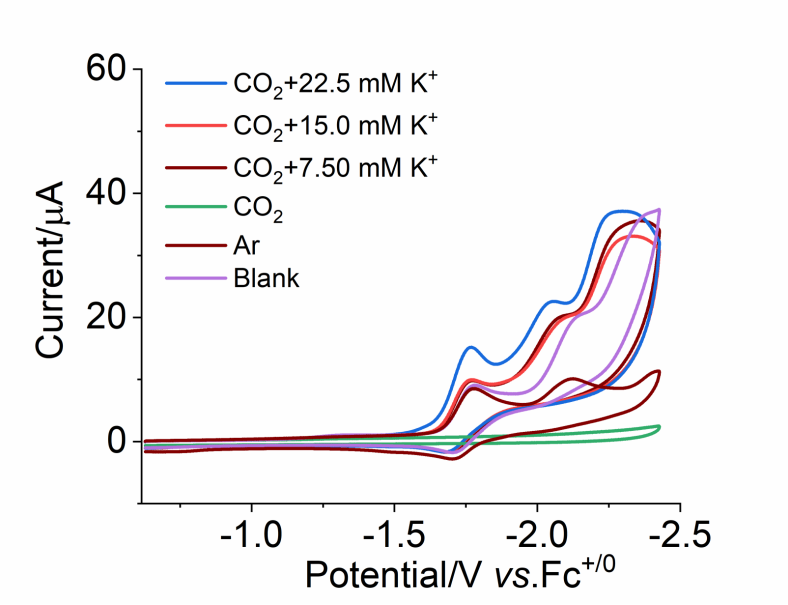

Figure S 52 CVs show 0.5 mM **1** with varied amounts of KPF_6 under CO_2. Voltammograms are taken at a scan rate of 100 mV/s with 0.1 M $^{n}Bu_4NPF_6$ in MeCN : DMF (4 : 1) solution. Glassy carbon working electrode, Ag^+/Ag reference electrode, and Pt wire counter electrode.

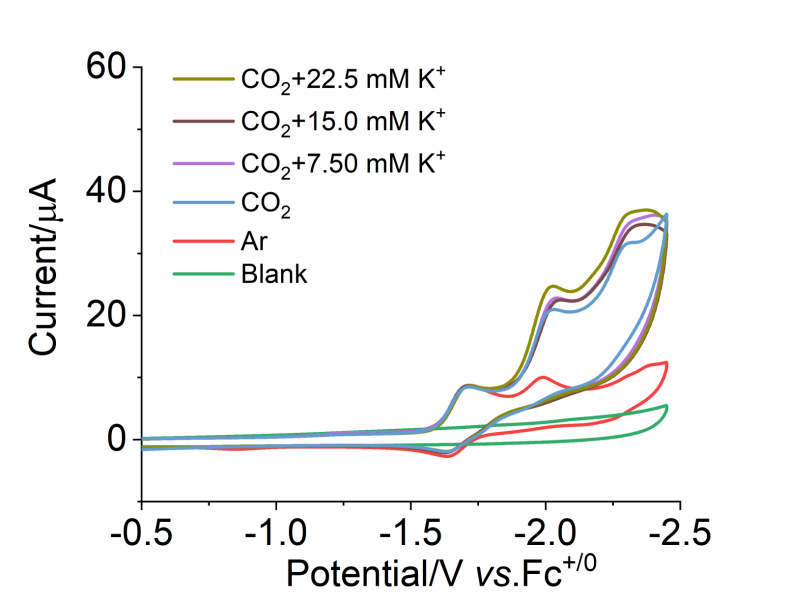

Figure S 53 CVs show 0.5 mM **2** with varied amounts of KPF_6 under CO_2. Voltammograms are taken at a scan rate of 100 mV/s with 0.1 M $^nBu_4NPF_6$ in MeCN : DMF (4 : 1) solution. Glassy carbon working electrode, Ag^+/Ag reference electrode, and Pt wire counter electrode.

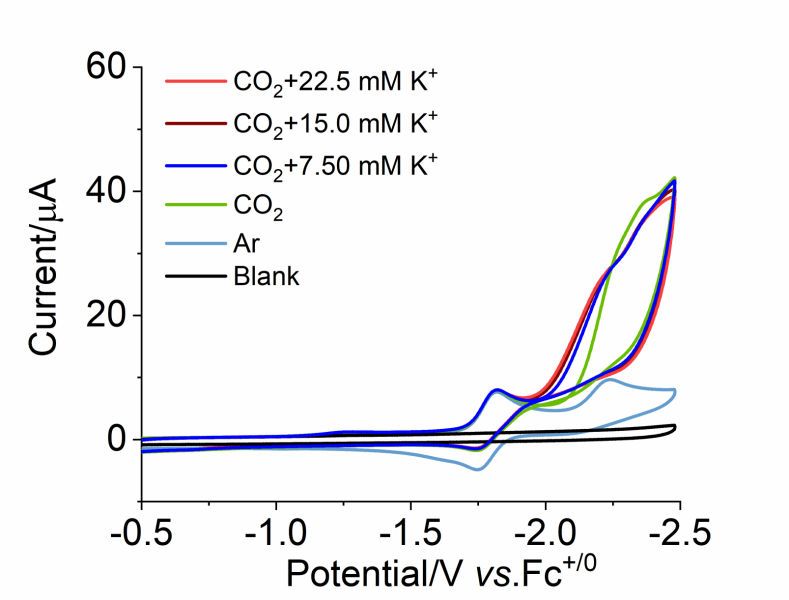

Figure S 54 CVs show 0.5 mM **3** with varied amounts of KPF_6 under CO_2. Voltammograms are taken at a scan rate of 100 mV/s with 0.1 M $^nBu_4NPF_6$ in MeCN : DMF (4 : 1) solution. Glassy carbon working electrode, Ag^+/Ag reference electrode, and Pt wire counter electrode.

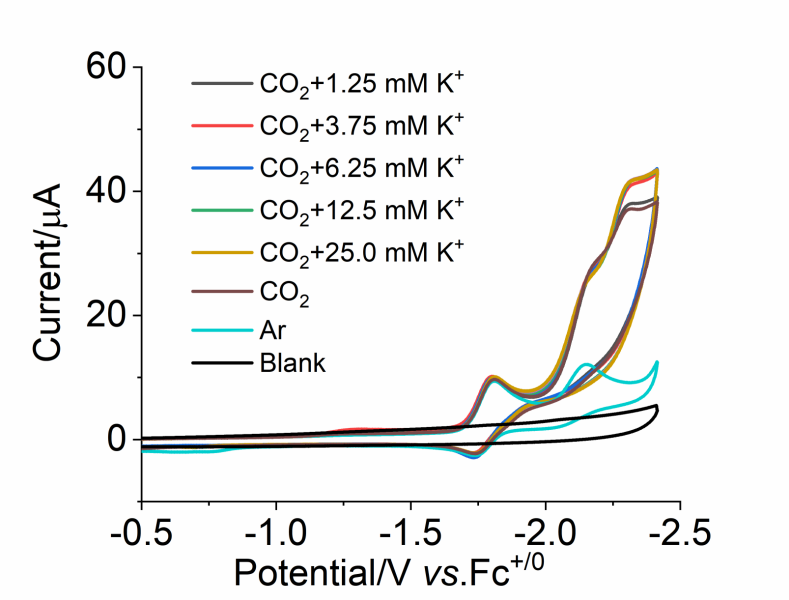

Figure S 55 CVs show 0.5 mM **4** with varied amounts of KPF_6 under CO_2. Voltammograms are taken at a scan rate of 100 mV/s with 0.1 M $^nBu_4NPF_6$ in MeCN : DMF (4 : 1) solution. Glassy carbon working electrode, Ag^+/Ag reference electrode, and Pt wire counter electrode.

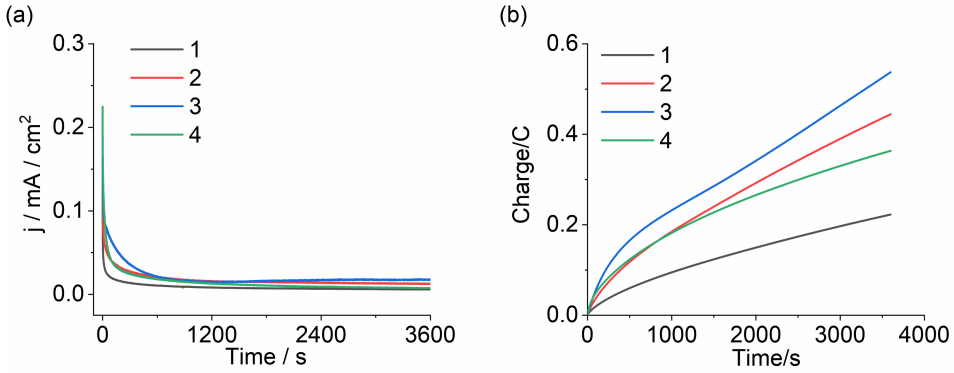

Figure S 56 (a) Controlled potential electrolysis at -2.25 *vs.* $Fc^{+/0}$ in the presence of 0.5 mM **1**-**4** and 25 mM KPF_6 under CO_2. (b) The charge integration after electrolysis for **1**-**4**. Voltammograms are taken at a scan rate of 100 mV/s with 0.1 M $^nBu_4NPF_6$ in MeCN : DMF (4 : 1) solution. Glassy carbon working electrode, Ag^+/Ag reference electrode, and Pt wire counter electrode.

Table S 6 The products selectivity of **1**-**4** in the same condition.

Complex (0.5 mM)	**1**	**2**	**3**	**4**	Blank
Potassium source (25 mM)	KPF_6	KPF_6	KPF_6	KPF_6	KPF_6
Potential / V *vs.* $Fc^{+/0}$	-2.25	-2.25	-2.25	-2.25	-2.25
Q / C	0.22	0.44	0.54	0.36	0.14
FE(CO) / (%)	39	77	45	70	0
H_2	0	0	0	0	/
TON	0.04	0.3	0.23	0.2	/

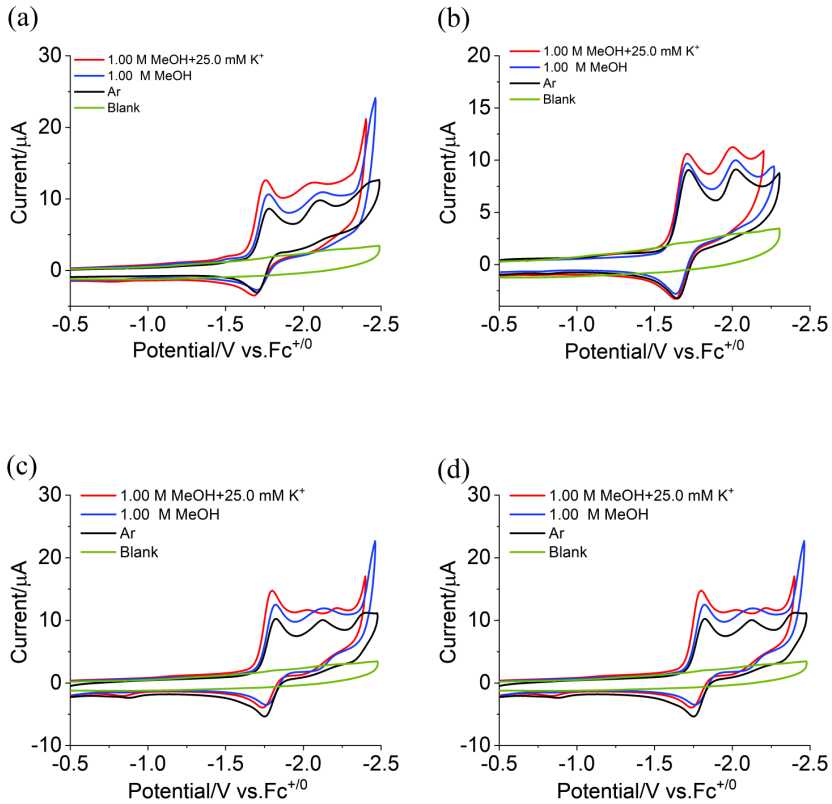

Figure S 57 (a) CVs show 0.5 mM **1** in the presence of 1 M methanol, upon addition of K^+ under Ar. (b) CVs show 0.5 mM **2** in the presence of 1 M methanol, upon addition of K^+ under Ar. (c) CVs show 0.5 mM **3** in the presence of 1 M methanol, upon addition of K^+ under Ar. (d) CVs show 0.5 mM **4** in the presence of 1 M methanol, upon addition of K^+ under Ar. Voltammograms are taken at a scan rate of 100 mV/s with 0.1 M ^{n}Bu$_4$NPF$_6$ in MeCN solution. Glassy carbon working electrode, Ag^+/Ag reference electrode, and Pt wire counter electrode.